Solid Earth Discuss., https://doi.org/10.5194/se-2019-43
Manuscript under review for journal Solid Earth
Discussion started: 27 March 2019

Solid Earth
Discussions

Evolution of a long-lived continental arc: a geochemical approach (Arequipa Batholith, Southern Peru)

Sophie Demouy[1], Mathieu Benoit[1*], Michel de Saint-Blanquat[1], Jérôme Ganne[1]

1 -, GET, OMP, Université Paul-Sabatier - CNRS - IRD, 14 avenue Edouard-Belin 31400 Toulouse, France.

*corresponding author: Mathieu.Benoit@get.omp.eu

ABSTRACT

Batholith emplacements within a continental margin may bear witness of a magmatic input lasting for several million years. Consequently, the geochemical signatures of such sections are complex, and their understanding in terms of petrological processes is crucial. The Arequipa section of the Coastal Batholith of Southern Peru was discontinuously constructed during several periods of magmatic activity, from the Jurassic to the Paleocene (200-175 Ma, and 90-60 Ma). Thermobarometric data on amphiboles indicates two main levels of emplacement at the batholith scale, the deepest between 5 and 7 km in depth and the second around 3.5 km. The present day outcropping of these different units at the same elevation argue for a large vertical movement along the Lluclla Fault System between 76 and 68 Ma. Both major/trace element contents and Nd-Sr isotopes show a large variability that is not random. The data dispersion is consistent with a two-stage evolutionary model of the magmatic arc, inspired by the MASH model: (i) an early stage dominated by hybridization and fractional crystallization processes, (ii) a late stage in which magmas were homogenized and mainly evolved by fractional crystallization. The change from one stage to another is controlled by the thermal state of the crustal arc section, especially the Deep Crustal Hot Zone.

Solid Earth Discuss., https://doi.org/10.5194/se-2019-43
Manuscript under review for journal Solid Earth
Discussion started: 27 March 2019

Solid Earth Discussions

Keywords: batholith, magmatic arc, Andes, granites, geochemistry, flair-up, MASH model

1. INTRODUCTION

Along active margins, subduction-related processes lead to the injection of voluminous calc-alkaline magmatic bodies into the continental crust. In general, only a small volumetric proportion of these magmas reach the surface as lavas (White et al., 2006). At intermediate and upper crustal levels, elongated plutonic bodies parallel to the trench are emplaced in composite batholiths. Their construction is spatially and temporally discontinuous, showing an alternation of high-flux episodes (HFE's) with magmatic lulls (Cruden and Mc Caffrey, 2001; Ducea, 2001; Haschke et al., 2002; Ducea and Barton, 2007; DeCelles et al., 2009; Bartley et al., 2008; Miller et al., 2011; Saint-Blanquat et al., 2011). HFE's are generally responsible for the generation of up to 75-80% of the arc volume within relatively short periods of 10-15 Ma. In the subduction setting, HFE events occurrence is linked to the development of a dense root and lower crust melting processes (DeCelles et al. 2009). Batholiths therefore provide an integrated picture of the evolution of long-lived subducting margin.

Petrological and geochemical studies on continental arc magmas reveal the protracted arc evolution reflected by the broad range in geochemical signatures within one composite batholith (Pankhurst et al. 1986; Wilson, M. 1989). Petrological processes related to the generation of intermediate and silicic arc magmas are 1) magma differentiation by fractional crystallization (Hamilton, 1983; Sisson and Layne, 1993; Müntener et al., 2001; Grove et al., 2002, 2003) and 2) contribution from the pre-existing continental crust. The contribution of at least one crustal component can occur following different processes; (i) through generation of crustal melts by partial melting of pre-existing ancient crust (Atherton and Petford, 1993; Tepper et al., 1993; Rapp, 1995) and/or younger mafic cumulates (Dungan and Davidson, 2004) around the mantle-crust transition, and successive mixing with juvenile primary magmas (ii) by crustal assimilation at various crust's levels, i.e AFC (DePaolo 1981; Powell 1984) or MASH (Hildreth and Moorbath 1988). Both processes are not mutually exclusive. Nevertheless, some authors are discussing the efficiency of the AFC process at middle-to

Solid Earth Discuss., https://doi.org/10.5194/se-2019-43
Manuscript under review for journal Solid Earth
Discussion started: 27 March 2019

shallow crustal levels, based on energetic considerations and geochemical modeling (Spera and Bohrson, 2001; Glazner, 2007; Clemens et al., 2009, 2010). A comprehensive model that integrates these different insights is the deep hot zone model proposed by Annen et al. (2006b). It provides a thermo-mechanical study that explains the generation of magmas derived by fractionation of high-pressure assemblages from both hydrous mantle-derived magmas and crustal liquids produced by partial melting.

The Andes is one of the two worldwide major orogens with Himalaya-Tibet, under which the continental crust currently reaches its maximal thickness. Several seismic studies estimated the crust to be 70 km-thick below the Central Andean Orocline (CAO, 13°S-28°S) and more precisely beneath the Western Cordillera, where the volcanic arc is located (Beck et al., 1996; James, 1971). The crustal thickening is hard to unravel over geological times, nevertheless it appears that the Andean crust underwent significant thinning prior to 90 Ma (Sempere et al., 2002), and slowly started its thickening from 90 Ma, before it significantly increased by 30 Ma (Mamani et al., 2010; Ganne et al., 2017).

In this paper, we intend to determine the evolution of a section of the Coastal Batholith of Peru, located in the area of Arequipa (16.5°S) through the Western Cordillera. This section is part of the more than 1600 km-long linear plutonic belt extending along the western margin of Peru (Pankhurst et al., 1986). The southern area of Peru is remarkable as: (i) No allochtonous terrane was accreted since the initiation of the subduction (570 Ma; Cawood 2005). (ii) The plutonic rocks are partly hosted by a thick Precambrian basement (Shackleton et al., 1979). It is also an area allowing the study of a long-lived arc history, and the interaction of arc magmas with an old basement. Moreover, the batholith of Arequipa represents a strong economic interest as it hosts an open-pit of copper and molybdenum mining complex (Cerro Verde Mine).

To document the geochemical evolution of this magmatic arc, we analysed major and traces elements (100 samples) and Sr and Nd isotopes (92 samples) were analyzed. We combined these data with ages obtained on the same sample set by in-situ U-Pb zircon method (Demouy et al., 2012). In the present study, we propose that the combination of both geochronological

Solid Earth Discuss., https://doi.org/10.5194/se-2019-43
Manuscript under review for journal Solid Earth
Discussion started: 27 March 2019

Solid Earth Discussions

data (U-Pb in-situ on zircon) and extensive geochemical studies (bulk rock major and trace elements and isotopic compositions) is a powerful approach to unravel the magmatic history of the arc system and to understand the contribution of the juvenile and/or crustal reservoirs in magmatic arc rocks.

2. GEOLOGICAL SETTING

The subduction along the Western coast of the South American plate is active since the beginning of the Paleozoic (570 Ma; Cawood 2005). Subduction-related magmatism led to the emplacement of granitic intrusions during the Ordovician (468-440 Ma; Loewy et al. 2004), the Carboniferous to Late Triassic period (325-215 Ma around Cuzco in the present Eastern Cordillera; Mišković et al. 2009) and during the Meso-Cenozoic. This study concerns the Liassic to Paleocene period in the Arequipa area.

The Costal Batholith of Peru is made up of more than 1000 plutons, extending over a 1600 km-long and 60 km-wide array, 150-200 km away from the present-day trench (Pankhurst et al., 1986). Close to the city of Arequipa, the plutonic rocks form the La Caldera complex (Stewart, 1968). They crop out from the Northwest towards the Southeast over nearly 1200 km^2, in which is located our studied area (80x60 km) (Figure 1). The La Caldera complex is made up of five principal plutonic units, and structured by three main faults (Le Bel 1985; Mukasa 1986a; Demouy, 2012; Demouy et al. 2012) (Figure 1). The Lluclla Fault System (LFS) is the largest accident, which divides the northwestern area of the batholith into northeastern and southwestern parts. The northeastern part is made of two plutonic units, intrusive into the Precambrian basement, the Gabbros & Diorites unit (GDU) and the Tiabaya unit (TU). Field relationship suggests a minimal thickness of 1 km for these units. The southwestern part corresponds to the Linga unit (LU), made up of an amalgam of several laccolith-shaped intrusions emplaced concordantly within the sedimentary Jurassic cover, and were tilted about 35° toward the SW after emplacement as indicated both by the bedding of the sedimentary country rocks and by the geometry of the contacts. This geometry indicates that the minimum thickness of this unit is around 8 km. Towards the southeast the

Solid Earth Discuss., https://doi.org/10.5194/se-2019-43
Manuscript under review for journal Solid Earth
Discussion started: 27 March 2019

Solid Earth
Discussions
Open Access
EGU

voluminous Yarabamba unit (YU) crops out both in the northeastern part and the southwestern part, postdating the Lluclla Fault System activity. At the southeastern extremity of the batholith section, the Chapi-Churajón unit (CCU) intrudes the basis of the sedimentary Jurassic cover. The different plutonic intrusions appear to be tabular-shaped, and each unit corresponds to an amalgamation of several intrusions as a result of a discontinuous magmatic activity that is a common feature in batholith sections (Saint Blanquat et al., 2011; Leuthold et al., 2012a).

Previous U-Pb geochronological studies conducted on zircon grains, either by ID-TIMS (Mukasa, 1986a) or in-situ LA-ICPMS (Demouy et al., 2012) indicates two main periods of activity of the magmatic arc in Arequipa. The first period occurred during the Jurassic, leading to the emplacement of the Gabbros & Diorites unit (200.0-175.8 Ma), of some intrusions in the southern part of the studied area (188.4 Ma) and of the Chapi-Churajón diorite (160.5 Ma). The second main period occurred during the Cretaceous-Paleocene (89.8 to 61.6 Ma), with the emplacement of the Tiabaya, the Linga, and the Yarabamba units. The emplacements of the Linga and Yarambamba units correspond to the latest period of activity of the arc (70-60 Ma) that leads to the construction of the largest volumes of the batholith (up to 75%). It was interpreted as a flare-up event at the batholith scale and a major contribution to the continental crust construction in this area (Demouy, 2012; Demouy et al., 2012).

The plutonic units intrude both the basement and a volcano-sedimentary cover. The basement is one of the several Proterozoic blocks cropping out in southern Peru and collectively named "the Arequipa Massif". Those rocks underwent complex, polycyclic magmatic and metamorphic history from the Early Proterozoic to the Early Paleozoic. First, a large orogenic cycle occurred between 2.1-1.8 Ga and then a second main one (Grenvillian event) between 1.2 and 0.97 Ga (Loewy et al., 2004; Casquet et al., 2010). In southern Peru, the Grenvillian event is described in the Camaná-Mollendo block between 1040 and 940 Ma (Martignole and Martelat, 2003; Casquet et al., 2010). The basement is overlain by a thick stratigraphic succession of Late Paleozoic to Neogene age, made of both volcanoclastic arc products and marine to continental sediments. The Paleozoic-Mesozoic part of this succession in the

Solid Earth Discuss., https://doi.org/10.5194/se-2019-43
Manuscript under review for journal Solid Earth
Discussion started: 27 March 2019

Solid Earth
Discussions
Open Access

Arequipa area is about 5 km-thick and is locally intruded by Jurassic to Paleogene intrusive rocks (Cruz, 2002; Sempere et al., 2002; Boekhout et al., 2013).

3. SAMPLING AND ANALYTICAL PROTOCOL

3.1 Sampling

The sampling was conducted following two rules: (i) take a large number of samples in each plutonic unit, (ii) avoid bias by sampling regularly each plutonic unit (maximum ~2km between each location) even if there is no field evidence of change in the mineralogy. We consider that this sampling strategy is well adapted to study both intra-and inter-plutonic petrological and geochemical variability. Sampling was mainly conducted along three main cross-sections, perpendicular to the NW-SE trend of the batholith. Intermediate and peripheral locations around the cross-sections were also sampled towards the NW, the SE and the southern parts of the study area (Figure 1). The location and main characteristics of each of the 100 samples selected for the geochemical study are listed in the Supplement A.

3.2 Analytical protocol

Quantitative analyses on mineral phases were performed at Université de Toulouse, GET (France) using a CAMECA SX50 microprobe with SAMx automation. The operating conditions were: accelerating voltage 15 kV, beam current 10nA or 20 nA (depending on the resistance of the mineral to beam damage) and analyzed surface 2x2 μm^2. Natural and synthetic minerals have been used as standards. Major and trace element abundances were acquired in SARM, Nancy (France) and ALS Mineral, Seville (Spain) by inductively coupled plasma atomic emission spectrometry (ICP-AES) and inductively coupled plasma mass spectrometry (ICP-MS) after LiBO2 fluxing. For isotopic measurement, we proceed to acid digestion (HNO_3-HF-H_2O_2) before evaporation and chemical separations. We used Eichrom Sr-SPEC and TRU-SPEC resins for Sr and REE elutions, respectively, and LN-SPEC resin for Nd elution. Sr, Nd isotopic ratios were measured using a Finnigan MAT-261 mass spectrometer. Repeated analyses of the NBS 987 standard yielded an average value of $^{87}Sr/^{86}Sr$ = 0.710238 ± 8 (2σ, n=7) with a standard deviation of 1.09x10-5. Repeated analyses of the La Jolla standard yielded an average value of $^{143}Nd/^{144}Nd$ = 0.511846 ± 6 (2σ, n=9) with a standard deviation of 6.01x10-6. The blank for Sr and Nd are negligible with quantities <200 pg for Sr and <50 pg for Nd.

4. PETROGRAPHY AND MINERAL CHARACTERISTICS

The plutonic units are defined through structural and petrological arguments. Each unit is made up of one or several plutons. In order to describe the different units we use the terminology defined by (Le Bel, 1985), who published the most detailed petrological study in this area. At the batholith's section scale, there are no large variations of the mineralogy for a given lithology from one unit to the other. Hence, to complete the general petrological observations by unit listed above, the characteristics of the main mineral phases are reported in Table 1.

• The Gabbros & Diorites unit is made of gabbros and diorites sensus lato (diorite and quartz-diorites, (Cox et al., 1979). The entire unit is located in the NE part of the batholith, and intrudes the Precambrian basement. It is locally affected by ductile and brittle deformations and is widely cut by thick (up to 10 m-wide), EW-trending, steeply dipping basaltic and granitic dykes. We identify amphibole-bearing and quartz-bearing gabbros. The average mineralogy for gabbros is Plg +Px +Amph +Ox ±Qz. One of the gabbroic samples corresponds to the oldest rock dated in the batholith (200.0 ± 1.2 Ma, Demouy et al. 2012). Some of the gabbros display cumulative textures with clinopyroxenes and plagioclases as cumulate phases (figure 2), and the other phases like amphibole and titanite are inter-cumulate phases. Diorites sensu stricto dominate the unit displaying a classical mineralogy: Plg ±Px +Amph +Bt ±Kf +Ox +Qz. The youngest age obtained in the Gabbros & Diorites unit corresponds to a quartz-diorite sample, which is the less represented facies (175.8 ± 1.2 Ma, Demouy et al. 2012).

Solid Earth Discuss., https://doi.org/10.5194/se-2019-43
Manuscript under review for journal Solid Earth
Discussion started: 27 March 2019

Solid Earth
Discussions
Open Access

• The Chapi-Churajón diorite is composed of two main intrusions. They both intrude the Jurassic sedimentary cover and are located at the most southeastern part of the studied area. The dioritic intrusion is located toward the southeast and the quartz-dioritic towards the northwest. The mineral assemblages of these two facies are uncommon at the batholith scale, characterized by the absence of amphibole and the occurrence of porphyritic K-feldspar (0.5-1.5 cm).

• The Tiabaya unit is made of two plutons (SE and NW), located in the northeastern part of the batholith. It mainly intrudes the Liassic component of the batholith (Gabbros & Diorites unit), and locally the Precambrian basement (Tiabaya-SE only). Each pluton is homogeneous considering the texture and the mineralogy of the rocks. Tiabaya NW is made of diorite and Tiabaya SE of quartz-diorite. Mineral assemblages are Plg ±Px +Amph +Bt +Ox +Kf +Sph +Zr. Ferro-magnesians minerals are euhedral and can reach several millimeters in the Tiabaya SE unit. Some amphiboles display clinopyroxene cores in the Tiabaya NW unit.

• The Linga unit is intrusive within the Jurassic sedimentary strata. It constitutes the southwestern part of the batholith and is made of several massive gabbrodioritic, dioritic, quartz-dioritic and granitic tabular bodies. As for the Gabbros & Diorites unit, the gabbros locally present cumulative characteristics. Diorites and quartz-diorites constitute the largest outcrops of the unit, and the granites are spatially restricted to the southwestern end of the San Jose Quebrada (Figure 1).

• The Yarabamba unit is mainly quartz-dioritic and intrudes the precambrian basement, the Chapi-Churajón diorite, the Tiabaya SE pluton, the Linga unit and the Jurassic sedimentary cover. The porphyry copper of the Cerro Verde Mine is associated with the micro-quartz-diorite facies of the Yarambamba unit, and a large part of the unit remains hidden under recent deposits. The Yarabamba unit is mainly made of quartz-diorites but we also identified some gabbro-diorites and granites scattered in the unit. Mineral assemblages for the quartz-diorite are similar to those of the Linga unit with Plg ±Amph +Bt +Ox +Kf.

Solid Earth Discuss., https://doi.org/10.5194/se-2019-43
Manuscript under review for journal Solid Earth
Discussion started: 27 March 2019

Solid Earth
Discussions

All the plutons of the studied area locally contain mafic enclaves and display magmatic fabrics and textures with rare clear evidences of magmatic foliation. They contain little evidences of post-emplacement deformation.

5. AMPHIBOLE THERMOBAROMETRY

We analyzed the amphibole grains of 16 samples from: basement (n: 1), Linga unit (n: 5), Tiabaya unit (n: 5) and Yarabamba unit (n: 1). The data are listed in Supplement B and plotted in Figure 3a and b and in figure 4 for P/T estimates. The range of temperature calculated is 904 to 662 C°, and the corresponding range of pressure is 3.3 to 0.4 kbar (Figure 4). The pressures correspond to upper crustal emplacement conditions (up to 13 km), and temperatures are consistent with those indicated in the literature for calk-alkaline magmas (Ridolfi and Renzulli, 2012). We observe both inter-and intra-plutonic units variations.

In Jurassic plutons, amphiboles indicate a 901-692˚C crystallization temperatures range for two different range of pressure: 1.9-1.0 kbar for the cumulative 09SD226 rock and 1.3-0.4 kbar for the 09SD221 and 09SD265 gabbros. The Cretaceous rocks are characterized by three different pressure ranges: (i) Linga 09SD012 (P: 0.9-0.7 kbar) (ii) Tiabaya 09SD31-33-34-164 (P: 1.6-1.1 kbar) (iii) Tiabaya 06SD160 mafic enclave (P: 3.5-1.2 kbar). Between theses three sets, the temperatures does not significantly differ and range from 829 to 662˚C. The Maastrichtian-Paleocene rocks constitute a homogeneous set of data (P: 1.0-0.5 kbar and T: 789-668˚C). The highest range of pressures corresponds to the amphiboles of the basement sample (3.5-2.2 kbar; T: 863-766˚C).

To sum up, we find three main ranges of pressure (i) a low range (P: 0.4-1.6 kbar) corresponding to the Gabbro & Diorite, Linga and Yarabamba units (ii) a middle range (P: 1.0-1.9 kbar) corresponding to the Tiabaya NW unit and a cumulative rock from Gabbro & Diorite unit. (iii) a high range (P : 1.2-4.5 kbar) corresponding to a mafic enclave in Tiabaya NW unit and the basement sample.

6. WHOLE ROCK GEOCHEMICAL DATA

6.1 *Major elements*

The major and trace element data is given in Supplement C. TAS diagram shows that the data are in good accordance with the petrographic description (Figure 5a). As a whole, samples from various periods of activity define trends that partly overlap themselves, fitting the calk-alkaline trend (Figure 5b). The six most mafic rocks (Gabbro & Diorite unit) that plot in the tholeiitic area are cumulative rocks, this explains their higher Fe content regarding the other samples. The A/CNK and A/NK molar ratios of the samples are negatively correlated, defining a large trend from the mafic to the felsic rocks (Figure 5c). Most of the sample set plot in the metaluminous area, and only the most evolved samples from the Jurassic rock set (quartz-diorites) and the Cretaceous granites display peraluminous affinities. Two samples are clearly peraluminous with A/CNK molar ratios >1.1, corresponding to two quartz-diorites from the Gabbro & Diorite unit, i.e. the youngest and the most differentiated rocks of this unit (09SD10 and 09SD27). The A/CNK ranges are high for for the Jurassic (0.66-1.21) and the Cretaceous (0.70-1.06) rocks, whereas for the Maastrichtian-Paleocene it is narrower (0.80-0.98). To sum up, according to the major elements, the sample set is made of three sample groups characteristic of typical of arc-magmatism that do not significantly differ as a function of their respective ages. Nevertheless, the youngest sample set (Maastrichtian-Paleocene) display less Major Element variations than the oldest sets.

6.2 Trace elements

As a whole, the trace elements patterns of our sample set are characteristics from arc-related Andean plutonic rocks (Figure 6 a and b).

The REE patterns of the entire sample set display common features with a light rare earth element (LREE)-enrichment (Figure 6a) and $(La/Yb)_N$ ratios ranging from 2.4 to 20.2. For each age group LREE fractionation increases with the differentiation degree of the rocks in similar proportion. For all samples, the $(La/Sm)_N$ ratio rises from gabbros and gabbro-diorites

Solid Earth Discuss., https://doi.org/10.5194/se-2019-43
Manuscript under review for journal Solid Earth
Discussion started: 27 March 2019

[$(La/Sm)_N$ = 1.4-4.4] through diorites and quartz-diorites [$(La/Sm)_N$ = 1.8-6.4] to granitic rocks [$(La/Sm)_N$ =2.7¬6.4]. The gabbros display lower normalized La and Yb values (La_N =9.8-89.4, Yb_N =2.9-14.9) than the diorites and quartz-diorites (La_N =37.9-189.4, Yb_N =6.3-21.7) and the granites (La_N =62.6-161.7, Yb_N =8.3-21.5). Surprisingly, the most enriched rocks belong to the dioritic group, and not the granite one. Two samples from the Gabbro & Diorite unit (09SD232) and the Lingua unit (09SD17) display strong positive Eu anomalies, with Eu/Eu* ratios >1.5, and are consistent with the cumulate textures mentioned in the petrological study. Indeed, plagioclase is one major phase in the mineralogy of these cumulative samples.

Except for the cumulative rocks, primitive mantle-normalized trace element patterns indicate similar geochemical characteristics for most of the rock types, and some differences appear in the relative size of the anomalies (Figure 6b). Most samples show positive anomalies in some LIL elements as Cs, Rb, U, Pb, Sr and also for Th and K, and relative depletions in HFS elements as Nb, Ta and also Ti and P. These features correspond to classical signatures of subduction-related magmas (McCulloch and Gamble, 1991). Nb negative anomaly is more pronounced in the intermediate and felsic rocks [granites: $(Nb/La)_N$ = 0.16-0.54)] than in the mafic rocks [gabbro-diorites : $(Nb/La)_N$ = 0.13-0.24)], as the negative Ti anomaly.

6.3 Sr and Nd isotopic data

Whole rock Sr and Nd isotopic data are reported in Supplement D along with Rb, Sr, Sm and Nd concentrations.

The $^{87}Sr/^{86}Sr_m$ range is large with values comprised between 0.70528 and 0.71788, as illustrated in the Rb-Sr isochron diagram (Figure 7). This figure highlights two different set of samples: (i) the first set is made of samples characterized by a narrow range of $^{87}Rb/^{86}Sr_c$ ratio (0.14-1.18) for a large range of $^{87}Sr/^{86}Sr_m$ ratio (0.70545-0.71279), with a scattered repartition. This domain includes all of the Jurassic samples (n: 20), the Cretaceous samples of the Tiabaya NW unit (n: 7), and several samples of the Yarabamba unit (n: 5). (ii) the second set contains

Solid Earth Discuss., https://doi.org/10.5194/se-2019-43
Manuscript under review for journal Solid Earth
Discussion started: 27 March 2019

samples characterized by a large range of both $^{87}Rb/^{86}Sr_c$ and $^{87}Sr/^{86}Sr_m$ ratio. The data align themselves, and these alignments are often interpreted as errorchrons in isochron diagrams. According to field, geochronological and geochemical data, all samples that fall along the calculated errorchrons are age-consistent (Figure 7). Therefore, we propose that these alignments do not correspond to mixing lines. The Cretaceous samples of the Lingua unit define three errorchrons (respectively estimated at 86, 88 and 89 Ma) that fall along a calculated Rb-Sr isochron calculated using U-Pb data from the sample 09SD275 (87.1 ± 1.0 Ma, $^{87}Sr/^{86}Sr_i$ = 0.70591): (i) the Linga-QLK group (n: 3), (ii) the Linga-SJK2 group (n: 6), (iii) the Linga-OPK group (n: 9). The Rb-Sr age's estimates are consistent with the U-Pb cretaceous ages previously obtained in this area (89.8 ± 0.7 Ma and 87.7 ± 1.0 Ma). The Maastrichtian-Paleocene samples (Linga-QLP, -SJP and -PAP, n: 23) fall along an 63.7 errorchron, which is consistent with the calculated Rb-Sr isochrones from samples 09SD318A, 09SD312, 09SD308 and 09SD18: respectively dated at 68.7 ± 0.5 and 65.5 ± 0.4 Ma (Demouy et al., 2012).

$^{143}Nd/^{144}Nd_m$ ratios range from 0.51208 to 0.51266, and their positioning in the Sm-Nd isochron diagram (Figure 8) is scattered, with no clear distinction between Jurassic, Cretaceous and Maastrichtian-Paleocene signatures. Nevertheless, the El Toro and Chapi-Churajón groups display higher $^{143}Nd/^{144}Nd_m$ ratios (0.51244-0.51266) than the Gabbro & Diorite unit (0.51224¬0.51260). We identify a set of 54 cretaceous and Maastrichtian-Paleocene samples concentrated within an area defined by $^{143}Nd/^{144}Nd_m$ values between 0.51244 and 0.51259 and $^{147}Sm/^{144}Nd_c$ values between 0.109 and 0.135. 9 samples plot outside of this area, corresponding to the Linga-QLK group (n: 3), 3 samples from the Yarabamba unit, 2 samples of the Linga-SJK1 group and 1 sample from the Tiabaya unit.

According to these results, we have performed age corrections for the measured samples. Two scenarios have been investigated: (i) samples that are falling on a single errorchron should have the same initial isotopic ratio. (ii) samples, which have been dated by U/Pb method should be corrected from their own ages, and for the other ones we use estimated ages (both errochrons or regional ages). We have decided to use option (ii) because option (i) is not applicable to Sm/Nd isotopic system and, for example, some of Maastrichtian-Paleocene samples that fall on the estimated errochron gave different U/Pb ages. Following this, initial isotopic ratios ranges are 0.70428 to 0.71095 for $^{87}Sr/^{86}Sr_i$ and 0.51202 to 0.51253 for $^{143}Nd/^{144}Nd_i$ (εNd from -10.4 to +1.71) for the whole dataset. They are reported in figure 9. Except for two jurassic samples from the El Toro area (related to the Ilo batholith), all samples plot in the crustal array and their positioning is significantly scattered. At a whole scale, we may observe a decrease of the scattering with time, pointing toward more juvenile signatures (Figure 9). This feature will be discussed in detail in the following sections.

7. DISCUSSION

7.1 Vertical movements during batholith emplacement

The Andes is one of the two worldwide major orogens with Himalaya-Tibet, under which the continental crust currently reaches its maximal thickness. Several seismic studies estimated the crust to be 70 km-thick below the Central Andean Orocline (CAO, 13°S-28°S) and more precisely beneath the Western Cordillera, where the volcanic arc is located (Beck et al., 1996; James, 1971). The crustal thickening is hard to unravel over geological times, nevertheless it appears that the Andean crust underwent significant thinning prior to 90 Ma (Sempere et al., 2002), and slowly started its thickening from 90 Ma, before it significantly increased by 30 Ma (Mamani et al., 2010).

In the Arequipa batholith, field and geochronological data constrain the timing and general organization of the plutonic units. Nevertheless, details on the functioning of the main accident affecting the batholith (Lluclla Fault System in particular) still remain a matter of debate. The movements linked to the faults have caused vertical displacements of the plutonic units that need to be quantified (Demouy et al., 2012).

The plutonic unit that currently crops out at the surface might have crystallized at different crustal depths, and granitoids barometry can play a critical role in constraining tectonic history (Smith et al., 1998). In the Arequipa batholith, the barometric data suggest two main levels of plutonic magma emplacement: a shallowest level (P: 0.4-1.6 kbar) for the Yarabamba, Linga and the Gabbros & Diorites units (apart from cumulate 09SD221), and a deepest level (P: 1.0-1.9 kbar) for the Tiabaya unit and the cumulative 09SD221 G&D sample. The amphiboles from the basement display higher crystallization pressures than in the plutonic units, attesting that the basement was exhumed before the pluton emplacement.

We observe both intra- and inter-plutonic unit discrepancies in terms of amphibole crystallization pressures. For the intra-plutonic unit variations: (i) within the Gabbros & Diorites unit, the gabbro 09SD221 and the related cumulative gabbro 09SD226 record different amphibole crystallization pressures. Results support the hypothesis of an early crystallization of some of the cumulative phases (1.6 kbar in average), rather than a complete magma differentiation at the batholith emplacement level (0.8 kbar in average); (ii) within the Tiabaya unit, highest amphibole crystallization pressures than in the surrounding dioritic samples characterize the large mafic enclave 09SD160. The enclave may have been extracted and dragged towards the surface by the dioritic magmas. The barometric data for the enclave range between 3.2 and 1.2 kbar supporting the idea of re-or syn-crystallization of amphiboles during the magma's ascent.

For the inter-plutonic unit variations: (i) The Jurassic rocks from G&D unit, apart from the cumulative one, correspond to the lower pressure range (P: 0.4-1.6 kbar) at the batholith scale. This unit (200 and 175 Ma, Demouy et al. 2012) crosscuts the basement of the Arequipa batholith. The emplacement depth of the magmatic unit is poorly constrained by the field observations. (ii) The Cretaceous rocks crop out both in the actual Northeastern part and the Southwestern part of the batholith, in the Tiabaya and the Linga units, respectively. The Cretaceous rocks emplaced at shallow (in the Southwestern part) or deeper crustal level (in Northeastern part), depending on their location.

According to the barometric data, the Tiabaya unit and the crosscutting Gabbros & Diorites unit did not emplace at the same level, and Cretaceous rocks emplaced at different depths on each side of the Lluclla faults System (Figure 10). Considerable crustal thinning occurred in

Solid Earth Discuss., https://doi.org/10.5194/se-2019-43
Manuscript under review for journal Solid Earth
Discussion started: 27 March 2019

Solid Earth
Discussions
Open Access

the Early Jurassic and culminated in the Middle Jurassic, leading to considerable subsidence in the Arequipa basin in southern Peru. This is shown by the accumulation of a 4500-6000-m-thick pile of Jurassic sediments (Yura Group, Sempere et al. 2002), covered by 500-1000-m-thick Cretaceous marine deposits. Hence, the Gabbros & Diorites unit that emplaced between 200 and 175 Ma at shallow level (P: 0.4-1.1 kbar) was buried during the Jurassic. At 90Ma, the thick sedimentary pile accumulated made possible different levels of emplacement for the Cretaceous arc magmas. In the Southwestern part, the magmas of the Linga unit emplaced between the Labra and Cachios formations, i.e. at approximately 3.5 km in depth. The amphiboles record pressures between 0.7 and 0.9 kbar. On the NE side of the Lluclla Fault System, the Tiabaya unit crosscuts the Gabbros & Diorites unit at a deeper level, with pressures ranging from 1.1 to 1.6 kbar. Following the estimation from the Linga unit, this indicates an emplacement level between 5-7 km. Starting at 69 Ma, the emplacement of the plutonic rocks occurred at the same level (Linga unit level), north and south of the Lluclla Fault System. This observation suggests that the northeast part of the batholith, that is the footwall of the Lluclla normal fault, was exhumed with a 1.5 to 3.5 km vertical movement in less than 10 Ma (between 76 and 68 Ma). The growth of the Coastal Batholith could be responsible of these extensional movements, which has to occur in a convergent geodynamic context. The emplacement of the Yarabamba unit clearly postdates the activity of the Lluclla Fault System at 66 Ma.

7.2 The geochemical variability of the Arequipa's batholith's magmas

7.2.1 Observations and questions

The geochemical signatures recorded by the igneous rocks of the Arequipa's section of the Coastal Batholith of Southern Peru show a broad diversity, which mimics what has been already observed in several other batholith sections (e.g. Sierra Nevada and Chilean batholiths; DePaolo 1981; Herve et al. 2007; Parada et al. 2007; DeCelles et al. 2009). The Jurassic, Cretaceous and Maastrichtian-Paleocene rocks of the Arequipa batholith section have the Nd and Sr isotopic compositions expected for subduction related igneous rocks (Figure 9). The data spread from the mantellic to the crustal quadrant, i.e. from the almost juvenile to strong crustal signatures. Each period of activity of the arc display different characteristics:

• Within the whole dataset, the Jurassic rocks display the largest $^{87}Sr/^{86}Sr_i$ and εNd ranges. On one side, the El Toro and Chapi-Churajón units display the most depleted, mantle-like signatures (εNd up to +1.7). On the other side, the Gabbros & Diorites unit displays a large range of $^{87}Sr/86Sr_i$, the highest value (0.71095) corresponding to the mafic oldest sample (gabbro 09SD221, 200.0 ± 1.1 Ma, Figure 9).

• The Maastrichtian to Paleocene rocks display a narrow range of isotopic signatures ($^{87}Sr/86Sr_i$ for Linga unit: 0.70516-0.70655), apart from three samples from the Yarabamba unit that were collected close to the borders of the unit.

• The Cretaceous rocks display intermediate isotopic signatures between the Jurassic and the Maastrichtian to Paleocene rocks. We observe a decrease in the isotopic heterogeneity starting from the oldest (Linga-SJK1) to the youngest (Tiabaya) samples. The youngest ones from the Tiabaya unit display the most juvenile signatures.

Besides the fact that a clear time gap exists between each plutonic unit emplacement episode, the isotopic variability tends to diminish with time and restricts itself in a domain located between the Ilo and the Upper Paleozoic Chilean areas in Figure 9. The simplest hypothesis would be that a different magmatic process characterizes each period of magmatic activity. However, there is an apparent paradox: the magmatic activity is discontinuous in the area, but if we consider all of the plutonic units as a whole; the more mafic, the more – isotopically - heterogeneous it is. This feature is the exact opposite to what the AFC process predicted (DePaolo, 1981). Given this paradox, the next section will address the two following questions:

1. Which process can explain the trace element and isotopic diversity encountered within each plutonic unit?

2. Why this heterogeneity becomes less and less pronounced in the youngest and more evolved samples?

Previous studies mentioned the broad geochemical diversity of the rocks from the southern Coastal Batholith of Peru (Tilton and Barreiro, 1980; Mukasa, 1986b; Boily et al., 1989) and underline the involvement of the Arequipa continental crust in the genesis of the arc magmas. However, it is at first glance difficult to vanish any juvenile input at the crust basis. Large chemical variations in worldwide batholithic rocks are commonly observed, and many different mechanisms have been considered to explain their acquisition. These mechanisms involve mixing/hybridization of magmas, and/or differentiation of the parental magmas (see review in Clemens and Stevens, 2012). They were at first envisioned at various crustal levels, from the depth closest to the magma source to higher levels in the uppermost magmatic systems. The most popular model to explain more particularly the isotopic variation in the batholiths is the AFC model (DePaolo, 1981) that combines the assimilation of the crustal wall-rock with the differentiation of the rocks. Because assimilation is energy consuming, these mechanisms might be more efficient at lower levels than at higher levels of the crust (Spera and Bohrson, 2001; Glazner, 2007).

7.2.2 Data exploration

Previous work on the Southern Peruvian Coastal Batholith proposed a two-step AFC model involving first a lower Precambrian crust and then a middle upper Precambrian crust - to explain the geochemical and isotopic diversity of the different plutonic rocks (Boily et al., 1989). Our dataset is clearly not consistent with an AFC model, as explained before. Moreover, regarding isotopes, several samples should have undergone excessive amount of combined assimilation and fractionation to explain their enriched signatures. This is inconsistent with their mafic compositions. In order to assess the questions listed before we have used Rb-Sr plots, in which we have reported the sample signatures (Figure 7). This approach allows us to draw some global sketches and isolate groups with specific elemental Rb/Sr ratios and Sr isotopic characteristics. They are listed hereafter:

Solid Earth Discuss., https://doi.org/10.5194/se-2019-43
Manuscript under review for journal Solid Earth
Discussion started: 27 March 2019

Solid Earth
Discussions

• The Maastrichian-Paleocene (MP) group includes 23 samples (diorites and quartz-diorites) issued from the Linga-QLP, -SJP and -PAP samples. Within this group, the samples cluster around a straight line. According to the U-Pb ages obtained on several samples from the MP-group (Maastrichtian-Paleocene ages, Demouy et al. 2012), we have superimposed on the data isochrones calculated from these ages. We observe that the distribution of the MP-group dataset fits with the domain defined by the calculated isochrones. This suggests that this trend corresponds to an errorchron and not to a mixing-line. The initial $^{87}Sr/^{86}Sr$ ratio indicated by the errochron (or whole rock isochron) is 0.705364 ± 0.000081.

• The Cretaceous (K) group includes the Linga -SJK2 (n: 3) and OPK samples (n: 8). Each dataset plots on a distinct trend. As for the MP-group, we calculated isochrones from the Cretaceous U-Pb ages of the Linga unit. The different trends are consistent with the calculated isochrones, and we consider them as errorchrons. Indeed, the two groups are consistent according to the field, geochemical and petrological observations.

• The O-group includes all the samples that do not spread along calculated isochrones (GDU, CCU, El Toro, TU, Linga-SJK1 and YU) . The $^{87}Sr/^{86}Sr_m$ range is large (0.70528-0.71228) for a small range of $^{87}Rb/^{86}Sr_c$ ratio (0.01-1.99). In this group we note the predominance of the mafic lithologies but also the occurrence of some quartz-diorites and granite.

We interpreted the trends obtained for the MP and K groups as errorchrons, as they fit with the calculated isochrones based on U-Pb zircon ages. According to this interpretation, the samples that plot along the same line share the same initial isotopic signatures. Then, variation along the $^{87}Rb/^{86}Sr_c$ axis may be considered at first glance as an effect of fractional crystallization, as 1) the increase of this ratio is a function of the biotite/plagioclase mineral cotectic proportions during magma evolution, and of their respective partition coefficients and 2) fractional crystallization alone do not affect the Sr isotopic ratio.

The three main groups identified in the Rb-Sr isochron diagram (Figure 9) are reported in several other plots: $^{87}Sr/^{86}Sr_i$, $^{143}Nd/^{144}Nd_i$ ratios, Lu and Sr concentrations, all plotted versus Zr concentrations (Figure 11), used as a fractionation index (FC, Pearce and Norry 1979, Figure D1). Between all the three groups, we can define two general sketches:

Solid Earth Discuss., https://doi.org/10.5194/se-2019-43
Manuscript under review for journal Solid Earth
Discussion started: 27 March 2019

• The K and MP-groups, which are characterized by a large range of Zr content (96 to 370 ppm), define the same trends. They have narrow ranges of initial $^{87}Sr/^{86}Sr_i$ (0.70481-0.70594) and $^{143}Nd/^{144}Nd_i$ (0.51237-0.51251) isotopic ratio. This is consistent with their respective position in the Rb-Sr isochron diagram (Figure 7). Relative to Zr, Lu correlates positively, Sr correlates negatively and initial $^{87}Sr/^{86}Sr$ and $^{143}Nd/^{144}Nd$ ratios remain constant. Therefore, there is no change in the isotopic signatures during magma differentiation, unlike what is predicted by AFC.

• Data from the O-group are characterized by lower Zr content (<200 ppm) and are much more scattered compared to the K and MP-groups. The O-group displays large ranges of $^{87}Sr/^{86}Sr_i$ (0.70388-0.71095) and $^{143}Nd/^{144}Nd_i$ (0.51202-0.51253) ratios. There is no linear correlation between the initial isotopic ratios and the fractionation index. Moreover, the scatter of the data seems to be less pronounced at high Zr abundances. This indicates that the more the magmas are evolved, the less – trace element content and isotopically speaking - heterogeneous they are.

Considering the entire set of data (MP, K, and O-groups), made of rocks of various ages, we observe a decrease in the chemical heterogeneity (both isotopic ratios and trace elements) with the increasing amount of Zr. The samples with Zr content higher than ± 200 ppm seem to share similar isotopic source. These features also suggest that different petrological processes dominate under and above the 200 ppm Zr content threshold.

7.2.3 Implication for the petrological processes

The MP-group. The MP-group is comprised of 23 samples, emplaced during a period of 8-Myr. This group can be described as isotopically homogeneous (Figure 9 and Figure 11). Processes like AFC, magma mixing/mingling or peritectic inheritance, if any, should have existed prior to the homogenization of the chemical signatures. As an example, the rocks have developed highly variable $^{87}Sr/^{86}Sr$ initial isotopic signatures because they were at first characterized by variable $^{87}Rb/^{86}Sr_c$ ratios. We propose that this ratio is at first order controlled by fractional crystallization. The rocks are linked with parental magmas that share common

Solid Earth Discuss., https://doi.org/10.5194/se-2019-43
Manuscript under review for journal Solid Earth
Discussion started: 27 March 2019

Solid Earth Discussions

geochemical features, and they underwent similar magmatic histories dominated by fractional crystallization.

The trends defined by the major and trace element data versus Zr abundances are consistent with this hypothesis, as are the field observations. Indeed, the structural organization of the Linga unit reveals that it was built as a superposition of several laccolith-shaped intrusions. This observation rules out the hypothesis that all samples from this group may come from a single, giant, melt batch that slowly cooled down and fractionated after emplacement. These laccoliths may then share a single parental magma reservoir that remained hot, stable and constantly fed at least during 8 Myr.

The initial isotopic signatures of this group are therefore the result of an homogenization process which happened before the replenishment of the parental magmatic reservoir. In this reservoir, the chemical signatures are neither purely crustal nor juvenile but intermediate.

The O-group. The O-group displays a broad isotopic, major and trace element heterogeneity. This heterogeneity tends to decrease as the Zr abundance in the rocks increases. These features call of several hypothesis concerning the genesis and evolution of the magmas. The contrasted isotopic signatures, especially for the lowest Zr content rocks, are consistent with the involvement of both crustal and juvenile sources. The range of isotopic signatures can be explained by various amounts of mixing between these two end members. We note that the scatter of the isotopic signatures is not in accordance with an AFC process, considering the mafic nature of some of the most radiogenic samples. Combined to this mixing process, fractionation occurs, giving a blend of rock types within the O-group (gabbros to quartz-diorites).

The acquisition of the geochemical heterogeneity is commonly considered to occur at two levels. Firstly, the source of the magmas may deliver a geochemical fingerprint to the partial melts. Secondly, the evolution of the magmas through processes like AFC leads to the dispersion of the initial isotopic ratios. These processes are not mutually exclusive. In our case, as there is no increase of the scatter in isotopic signatures towards the most evolved melts, we consider that the AFC process does not dominate the evolution of the magmas. The

Solid Earth Discuss., https://doi.org/10.5194/se-2019-43
Manuscript under review for journal Solid Earth
Discussion started: 27 March 2019

chemical variability of the mafic end-members reflect the heterogeneity of the source, and the more the melts fractionated, the less they differ from an isotopic point of view (Voshage et al., 1990).

The initial chemical heterogeneity inherited from the source suggests a gradual homogenization of the residual magmas as fractionation proceeds, until the melts reach 200 ppm Zr content.

The K-group. The K-group presents geochemical similarities with the MP-group, especially in terms of isotopic signatures: initial $^{87}Sr/^{86}Sr$ and $^{143}Nd/^{144}Nd$ ratios are rather consistent within this group. Fractionation is the primary process that controls the sample signatures within this group. We note that 4 samples from the K-group are characterized by 100 ppm Zr content, which is rather low. The [Sr] and [Lu] versus [Zr] content plot (Figure 11) suggest that these 4 samples evolved within an isolated batch, which is consistent with the field data (samples come from the Linga unit, with ages between 90 -87 Ma, Demouy et al. 2012).

Again, despite the various ages and the various plutonic units, there is a consistent scheme within the geochemical signatures of the samples in the Arequipa area. The first stage ([Zr] <200 ppm) is dominated by both mixing and fractionation, and the second stage ([Zr] >200 ppm) is mostly dominated by fractionation only, starting from a homogeneous primary reservoir. Are these assumptions consistent with what we know about the costal Batholith history?

7.3 The evolution of the geochemical signature through time: a geodynamical control?

As within several active margins, the magmatic activity in the margin of Southern Peru is discontinuous during the Mesozoic and the Cenozoic (Dallmeyer et al., 1996; Coleman and Glazner, 1997; Ducea, 2001; Lucassen et al., 2002; Parada et al., 2005; DeCelles et al., 2009; Demouy et al., 2012). The emplacement of the plutonic rocks through time is a record of the magmatic arc localization, alternatively trenchward and landward (Mamani et al., 2008; Demouy et al., 2012). This movement is linked to the global geodynamic context: from at least the late Permian, the active margin of Southern Peru is experiencing an extensive regime.

This leads to an important crustal thinning that started in the Early Jurassic and culminated in the Middle Jurassic (Sempere et al., 2002). The arc migrates trenchward from 200 to at least 150 Ma. This extension stops during the Early Cretaceous before westward drifting after the Cenomanian (Somoza and Zaffarana, 2008). During this period, the arc migrates landward and impinged the Arequipa area from 90 to at least 60 Ma.

Plate tectonic considerations have strong implications for the magma genesis and emplacement in this specific geodynamic environment. Considering the theoretical MASH model (Hildreth and Moorbath, 1988) and its recent support through numerical models (Annen et al., 2006b), we suggest that deep crustal hot zones are areas where the geochemical signatures of the magmas are acquired. Several studies attest that the accumulation of silicic magmas in a relatively cold and brittle environment favors eruption over accumulation, while later magmas accumulation in a warm ductile crust favors accumulation over eruption (Jellinek and DePaolo, 2003; de Silva et al., 2006a and b; Bachmann et al., 2007).

In the Arequipa area we identify two contrasted tectonic contexts during the magmatic arc activity in Arequipa: (i) initiation and protracted magmatic activity within a thinned Jurassic crust (200-175 Ma) (ii) initiation and protracted magmatic activity within a thickening crust, from the Late Cretaceous to the Maastrichtian-Paleocene (90-60 Ma).

We can link the geochemical groups (O-K-and MP-) with these two situations. The O-group is mainly composed of Jurassic rocks and some of the oldest Cretaceous rocks of Linga and the Tiabaya unit. It corresponds to stage (i) and part of stage (ii). The O-group melts did not evolve in a thickened crust. The K-group and MP-group correspond to the protracted activity of stage (ii), i.e. the evolution of the magmatic activity within a hot crust being thicken.

The initiation of magmatic activity at the base of the crust may trigger the emplacement of a certain amount of juvenile magma around the crust/mantle boundary. These magmas quickly crystallize at first, but the gradual heating of the deep crustal hot zone allows the production of various magma batches, characterized by various amounts of crustal input. This stage corresponds to the Mixing and Assimilation processes from the MASH model. In Arequipa, the Jurassic magmas (Gabbros & Diorites, El Toro and Chapi-Churajón plutons) are characterized by large geochemical heterogeneities, especially in the isotopic signal. Plutonic bodies are relatively small compared to the Jurassic volcanic and volcanoclastic deposits in Southern Peru (up to 6 km-thick, Chocolate Formation, Boekhout et al. 2013). The protracted magmatic activity from 200 to 175 Ma in Arequipa was not sufficient to thicken the crustal arc section, as the active margin was subject to an important crustal thinning during this period (Sempere et al., 2002). Hence, the crust do not reach a mature thermal state, but the gradual heating of the deep crust system still triggered partial homogenization of the magmas (O-group between 0 and 200 ppm Zr content). The petrological processes that dominate in this case are mixing and fractional crystallization.

Around 90 Ma, the reactivation of the magmatic activity below a cold crust leads to similar plutonic body emplacements: they are small in size and do present contrasted isotopic signatures (Linga-SJK1 and Tiabaya groups). These characteristics then changed. The active margin is no longer under extensional regime, allowing the thickening of the crust below the magmatic arc. This thickening leads to the development of a deep hot crustal zone that reaches a "mature" thermal state. This situation favors magma storage and homogenization at great depth, from a simple buoyancy point of view. Numerical models attest that silica-rich magmas can be generated by incomplete crystallization of hydrous basalts in the deep crust (Müntener et al., 2001; Prouteau and Scaillet, 2003). Hence the thermal maturation of the arc system allows the generation of more differentiated magmas that are submitted to Storage and Homogenization (MASH model). This evolution leads to the emplacement of large plutonic bodies at the batholith level, which are mainly subject to magmatic fractionation. These bodies are sharing common primitive parental melts, located at a deep level in a single, homogeneous, reservoir (K-and MP-group). The MP-group is symptomatic of this system: from 70 to 60 Ma, thousands of km^3 of magmatic liquids are produced, all sharing the same source; it is defined as a flare-up event. It is worth noting that this period is characterized by large ignimbritic explosions at the surface, which may be intrinsically linked to this process (in Southern Peru, Paralaque Formation, Bellido and Guevara 1963; Martinez and Cervantes 2003).

Solid Earth Discuss., https://doi.org/10.5194/se-2019-43
Manuscript under review for journal Solid Earth
Discussion started: 27 March 2019

Solid Earth
Discussions

8. CONCLUSIONS

The Arequipa batholith is made up of several plutonic units that record a long subduction-related discontinuous magmatic activity from the Jurassic to the Paleocene (200-175 and 90-60 Ma). The various plutonic units display a large geochemical heterogeneity at the batholith scale that are consistent with the signatures reported for plutonic rocks in magmatic arcs. Both field observations and barometric calculations obtained on amphibole phases allow to identify several vertical movements during the batholith emplacement, especially linked to the main Lluclla Fault System. The Jurassic rocks from the Gabbros & Diorites unit emplaced at shallow depth (0.8 kb in average), before being buried under a thick sedimentary cover during the crustal thinning affecting the entire active margin of Southern Peru. The reactivation of the magmatic activity during the Late Cretaceous leads to the emplacement of plutonic rocks at two different levels: the Tiabaya unit emplaced through the Gabbros & Diorites unit at a deeper level (5-7 km depth) than the Linga unit (3.5 km depth). These two plutonic units are currently located at the same elevation and are separated by the Lluclla Fault System. We propose that this Fault System activation leads to the raising of the Tiabaya unit between 76 and 68 Ma. This is confirmed by the fact that Maastrichtian-Paleocene rocks cropping out on both sides of the Lluclla Fault System display the same amphibole crystallization pressure.

The geochemical signatures of the plutonic rocks of the Arequipa batholith display a large heterogeneity within the mafic samples, and we observe a tendency for homogenization linked to fractionation. We propose a two-stage evolution model for the magmatic arc in the Arequipa area. The first stage consists in the initiation of the magmatic activity that leads to the emplacement of disconnected, mafic, small and isotopically heterogeneous plutons. This stage is due to the domination of mixing and fractional crystallization petrological processes in the deep crust, and lasts as long as the crustal arc section cannot thicken and reach a thermal maturity threshold. In Arequipa, the crustal thinning that occurs during the Jurassic period prevents from reaching this maturity. The switch to a convergent geodynamical context from the Early Cretaceous allows the thickening of the arc crust section. The second stage is reached when the crust has thickened enough to allow the development of a deep hot crustal zone where the petrological processes of homogenization and fractional crystallization are dominant. During this second stage, the softening of the crust at several levels allows the formation of deep magmatic reservoirs from which numerous magmas batches rise to emplace as voluminous plutons at the batholith level. The paroxysm of this system leads to the occurrence of flare-up events, and to the concomitant emplacement of the largest plutonic units and major ignimbritic explosions.

FUNDING

The project was supported by the Institut de Recherche pour le Développement and the Institut National des Sciences de l'Univers - CNRS SYSTER program.

ACKOWLEDGEMENTS

We thank Georges Ceuleneer for his careful rereading, Pierre Brunet, Jonathan Prunier and Manuel Henry for the technical assistance. The Sociedad Minera Cerro Verde S.A.A has allowed a significant part of the field studies.

REFERENCES

Anders, E. and Grevesse, N. : Abundances of the elements: meteoric and solar. Geochimica et Cosmochimica Acta 53: 197-214, 1989.

Annen, C., Blundy, J. D. and Sparks, R. S. J.: The Genesis of Intermediate and Silicic Magmas in Deep Crustal Hot Zones, J Petrology, 47(3), 505–539, doi:10.1093/petrology/egi084, 2006.

Atherton, M. and Petford, N.: Generation of Sodium-Rich Magmas from Newly Underplated Basaltic Crust, Nature, 362(6416), 144–146, doi:10.1038/362144a0, 1993.

Bachmann, O., Miller, C. F. and de Silva, S. L.: The volcanic-plutonic connection as a stage for understanding crustal magmatism, J. Volcanol. Geotherm. Res., 167(1–4), 1–23, doi:10.1016/j.jvolgeores.2007.08.002, 2007.

Bartley, J. M., Coleman, D. S. and Glazner, A. F.: Incremental pluton emplacement by magmatic crack-seal, Trans. R. Soc. Edinb.-Earth Sci., 97, 383–396, doi:10.1017/S0263593300001528, 2006.

Beck, S. L., Zandt, G., Myers, S. C., Wallace, T. C., Silver, P. G. and Drake, L.: Crustal-thickness variations in the central Andes, Geology, 24(5), 407–410, doi:10.1130/0091-7613(1996)024<0407:CTVITC>2.3.CO;2, 1996.

Solid Earth Discuss., https://doi.org/10.5194/se-2019-43
Manuscript under review for journal Solid Earth
Discussion started: 27 March 2019

Bel, L.: Mineralization in the Arequipa segment: the porphyry-Cu deposit of Cerro Verde/Santa Rosa., in Magmatism at a plate edge. The Peruvian Andes, Blackie Halsted Press, Glasgow and London., 1985.

Bellido Bravo, E. and Guevara Rosillo, C.: Geología de los cuadrángulos de Punta de Bombón y Clemesí 35-s y 35-t - [Boletín A 5], Instituto Geológico, Minero y Metalúrgico. 1963.

Boekhout, F., Sempere, T., Spikings, R. and Schaltegger, U.: Late Paleozoic to Jurassic chronostratigraphy of coastal southern Peru: Temporal evolution of sedimentation along an active margin, J. South Am. Earth Sci., 47, 179–200, doi:10.1016/j.jsames.2013.07.003, 2013.

Boily, M., Brooks, C., Ludden, J. and James, D.: Chemical and Isotopic Evolution of the Coastal Batholith of Southern Peru, Journal of Geophysical Research-Solid Earth and Planets, 94(B9), 12483–12498, doi:10.1029/JB094iB09p12483, 1989.

Casquet, C., Fanning, C. M., Galindo, C., Pankhurst, R. J., Rapela, C. W. and Torres, P.: The Arequipa Massif of Peru: New SHRIMP and isotope constraints on a Paleoproterozoic inlier in the Grenvillian orogen, J. South Am. Earth Sci., 29(1), 128–142, doi:10.1016/j.jsames.2009.08.009, 2010.

Cawood, P. A.: Terra Australis Orogen: Rodinia breakup and development of the Pacific and Iapetus margins of Gondwana during the Neoproterozoic and Paleozoic, Earth-Sci. Rev., 69(3–4), 249–279, doi:10.1016/j.earscirev.2004.09.001, 2005.

Clemens, J. D. and Stevens, G.: What controls chemical variation in granitic magmas?, Lithos, 134, 317–329, doi:10.1016/j.lithos.2012.01.001, 2012.

Clemens, J. D., Darbyshire, D. P. F. and Flinders, J.: Sources of post-orogenic calcalkaline magmas: The Arrochar and Garabal Hill-Glen Fyne complexes, Scotland, Lithos, 112(3–4), 524–542, doi:10.1016/j.lithos.2009.03.026, 2009.

Clemens, J. D., Helps, P. A. and Stevens, G.: Chemical structure in granitic magmas - a signal from the source?, Earth Environ. Sci. Trans. R. Soc. Edinb., 100, 159–172, doi:10.1017/S1755691009016053, 2010.

Coleman, D. S. and Glazner, A. F.: The Sierra Crest magmatic event: Rapid formation of juvenile crust during the Late Cretaceous in California, edited by W. G. Ernst and C. A. Nelson, Bellwether Publishing, Ltd, Columbia, 1998.

Cox, K. G., Bell, J. D. and Pankhurst, R. J.: The interpretation of igneous rocks, 1st ed., repr., Chapman & Hall, London., 1993.

Cruden, A. R. and McCaffrey, K. J. W.: Growth of plutons by floor subsidence: Implications for rates of emplacement, intrusion spacing and melt-extraction mechanisms, Phys. Chem. Earth Pt. A-Solid Earth Geod., 26(4–5), 303–315, doi:10.1016/S1464-1895(01)00060-6, 2001.

Cruz, M.: Estratigrafía y evolutión tectono-sedimentaria de los depósitos sin-orogénicos del cuadrángulo de Huambo (32-r, Cuadrante-II): Las formaciones Ashua y Huanca. Departamento de Arequipa, PhD, Universidad Nacional San Augustin de Arequipa., 2002.

Dallmeyer, R. D., Brown, M., Grocott, J., Taylor, G. K. and Treloar, P. J.: Mesozoic magmatic and tectonic events within the Andean plate boundary zone, 26 degrees-27 degrees 30'S, North Chile: Constraints from Ar-40/Ar-39 mineral ages, J. Geol., 104(1), 19–40, doi:10.1086/629799, 1996.

De Silva, S., Silva, S. D., Zandt, G., Trumbull, R., Viramonte, J. G., Salas, G. and Jimenez, N.: Large ignimbrite eruptions and volcano-tectonic depressions in the Central Andes: a

Solid Earth Discuss., https://doi.org/10.5194/se-2019-43
Manuscript under review for journal Solid Earth
Discussion started: 27 March 2019

Solid Earth
Discussions

thermomechanical perspective, Geological Society, London, Special Publications, 269(1), 47–63, n.d.

DeCelles, P. G., Ducea, M. N., Kapp, P. and Zandt, G.: Cyclicity in Cordilleran orogenic systems, Nat. Geosci., 2(4), 251–257, doi:10.1038/NGEO469, 2009.

Demouy, S.: La naissance des Andes au Crétacé supérieur□: origine et construction du Batholite Côtier sud-péruvien (Région d'Arequipa), Thèse d'Université, Université Paul Sabatier, Toulouse, 2012.

Demouy, S., Paquette, J.-L., de Saint Blanquat, M., Benoit, M., Belousova, E. A., O'Reilly, S. Y., Garcia, F., Tejada, L. C., Gallegos, R. and Sempere, T.: Spatial and temporal evolution of Liassic to Paleocene arc activity in southern Peru unraveled by zircon U-Pb and Hf in-situ data on plutonic rocks, Lithos, 155, 183–200, doi:10.1016/j.lithos.2012.09.001, 2012.

DePaolo, D. J.: A neodymium and strontium isotopic study of the Mesozoic calc-alkaline granitic batholiths of the Sierra Nevada and Peninsular Ranges, California, Journal of Geophysical Research: Solid Earth, 86(B11), 10470–10488, doi:10.1029/JB086iB11p10470, 1981.

Ducea, M.: The California Arc: Thick Granitic Batholiths, Eclogitic Residues, Lithospheric-Scale Thrusting, and Magmatic Flare-Ups, GSA TODAY, 7, 2001.

Ducea, M. N. and Barton, M. D.: Igniting flare-up events in Cordilleran arcs, Geology, 35(11), 1047–1050, doi:10.1130/G23898A.1, 2007.

Dungan, M. A. and Davidson, J.: Partial assimilative recycling of the mafic plutonic roots of arc volcanoes: An example from the Chilean Andes, Geology, 32(9), 773–776, doi:10.1130/G20735.1, 2004.

Ganne, J., Schellart, W., Rosenbaum, G., Feng, X. and de Andrade, V.: Probing crustal thickness evolution and geodynamic processes in the past from magma records: An integrated approach, GSA Special Paper, 526, DOI :10.1130/2017.2526(01), 2017.

Glazner, A. F.: Thermal limitations on incorporation of wall rock into magma, Geology, 35(4), 319–322, doi:10.1130/G23134A.1, 2007.

Grove, T. L., Parman, S. W., Bowring, S. A., Price, R. C. and Baker, M. B.: The role of an H2O-rich fluid component in the generation of primitive basaltic andesites and andesites from the Mt. Shasta region, N California, Contrib. Mineral. Petrol., 142(4), 375–396, doi:10.1007/s004100100299, 2002.

Grove, T. L., Elkins-Tanton, L. T., Parman, S. W., Chatterjee, N., Muntener, O. and Gaetani, G. A.: Fractional crystallization and mantle-melting controls on calc-alkaline differentiation trends, Contrib. Mineral. Petrol., 145(5), 515–533, doi:10.1007/s00410-003-0448-z, 2003.

Hamilton, W.: Orogenic Andesites and Plate-Tectonics - Gill,jb, Am. J. Sci., 283(6), 633–634, 1983.

Haschke, M., Siebel, W., Gunther, A. and Scheuber, E.: Repeated crustal thickening and recycling during the Andean orogeny in north Chile (21 degrees-26 degrees S), J. Geophys. Res.-Solid Earth, 107(B1), 3019, doi:10.1029/2001JB000328, 2002.

Herve, F., Pankhurst, R. J., Fanning, C. M., Calderon, M. and Yaxley, G. M.: The South Patagonian batholith: 150 my of granite magmatism on a plate margin, Lithos, 97(3–4), 373–394, doi:10.1016/j.lithos.2007.01.007, 2007.

Hildreth, W. and Moorbath, S.: Crustal Contributions to Arc Magmatism in the Andes of Central Chile, Contrib. Mineral. Petrol., 98(4), 455–489, doi:10.1007/BF00372365, 1988.

James, D. E.: Andean crustal and upper mantle structure, Journal of Geophysical Research (1896-1977), 76(14), 3246–3271, doi:10.1029/JB076i014p03246, 1971.

Jellinek, A. M. and DePaolo, D. J.: A model for the origin of large silicic magma chambers: precursors of caldera-forming eruptions, Bull. Volcanol., 65(5), 363–381, doi:10.1007/s00445-003-0277-y, 2003.

Le Bel, L.: Mineralization in the Arequipa segment: the porphyry-Cu deposit of Cerro Verde/Santa Rosa, edited by Pitcher W.S., Atherton M.P., Cobbing E.J. et Beckinsale E.R.D., Magmatism at a plate edge, The Peruvian Andes, Blackie Halsted Press, Glasgow and London, 1985.

Leuthold, J., Muentener, O., Baumgartner, L. P., Putlitz, B., Ovtcharova, M. and Schaltegger, U.: Time resolved construction of a bimodal laccolith (Torres del Paine, Patagonia), Earth Planet. Sci. Lett., 325, 85–92, doi:10.1016/j.epsl.2012.01.032, 2012.

Loewy, S. L., Connelly, J. N. and Dalziel, I. W. D.: An orphaned basement block: The Arequipa-Antofalla basement of the central Andean margin of South America, Geol. Soc. Am. Bull., 116(1–2), 171–187, doi:10.1130/B25226, 2004.

Lucassen, F., Escayola, M., Romer, R. L., Viramonte, J., Koch, K. and Franz, G.: Isotopic composition of Late Mesozoic basic and ultrabasic rocks from the Andes (23–32°S) – implications for the Andean mantle, Contrib Mineral Petrol, 143(3), 336–349, doi:10.1007/s00410-001-0344-3, 2002.

Mamani, M., Tassara, A. and Woerner, G.: Composition and structural control of crustal domains in the central Andes, Geochem. Geophys. Geosyst., 9, Q03006, doi:10.1029/2007GC001925, 2008.

Mamani, M., Woerner, G. and Sempere, T.: Geochemical variations in igneous rocks of the Central Andean orocline (13 degrees S to 18 degrees S): Tracing crustal thickening and magma generation through time and space, Geol. Soc. Am. Bull., 122(1–2), 162–182, doi:10.1130/B26538.1, 2010.

Martignole, J. and Martelat, J. E.: Regional-scale Grenvillian-age UHT metamorphism in the Mollendo-Camana Block (basement of the Peruvian Andes), J. Metamorph. Geol., 21(1), 99–120, doi:10.1046/j.1525-1314.2003.00417.x, 2003.

Matzel, J. E. P., Bowring, S. A. and Miller, R. B.: Time scales of pluton construction at differing crustal levels: Examples from the Mount Stuart and Tenpeak intrusions, North Cascades, Washington, Geol. Soc. Am. Bull., 118(11–12), 1412–1430, doi:10.1130/B25923.1, 2006.

Mcculloch, M. and Gamble, J.: Geochemical and Geodynamical Constraints on Subduction Zone Magmatism, Earth Planet. Sci. Lett., 102(3–4), 358–374, doi:10.1016/0012-821X(91)90029-H, 1991.

Miller, C. F., Furbish, D. J., Walker, B. A., Claiborne, L. L., Koteas, G. C., Bleick, H. A. and Miller, J. S.: Growth of plutons by incremental emplacement of sheets in crystal-rich host: Evidence from Miocene intrusions of the Colorado River region, Nevada, USA, Tectonophysics, 500(1–4), 65–77, doi:10.1016/j.tecto.2009.07.011, 2011.

Miskovic, A., Spikings, R. A., Chew, D. M., Kosler, J., Ulianov, A. and Schaltegger, U.: Tectonomagmatic evolution of Western Amazonia: Geochemical characterization and zircon U-Pb geochronologic constraints from the Peruvian Eastern Cordilleran granitoids, Geol. Soc.

Am. Bull., 121(9–10), 1298–1324, doi:10.1130/B26488.1, 2009.

Mukasa, S.: Common Pb Isotopic Compositions of the Lima, Arequipa and Toquepala Segments in the Coastal Batholith, Peru - Implications for Magmagenesis, Geochim. Cosmochim. Acta, 50(5), 771–782, doi:10.1016/0016-7037(86)90353-4, 1986a.

Mukasa, S.: Zircon U-Pb Ages of Super-Units in the Coastal Batholith, Peru - Implications for Magmatic and Tectonic Processes, Geol. Soc. Am. Bull., 97(2), 241–254, doi:10.1130/0016-7606(1986)97<241:ZUAOSI>2.0.CO;2, 1986b.

Muntener, O., Kelemen, P. B. and Grove, T. L.: The role of H2O during crystallization of primitive arc magmas under uppermost mantle conditions and genesis of igneous pyroxenites: an experimental study, Contrib. Mineral. Petrol., 141(6), 643–658, 2001.

Pankhurst, R. J.: W. S. Pitcher, M. P. Atherton, E. J. Cobbing and R. D. Beckinsale., eds. Magmatism at a Plate Edge: the Peruvian Andes. Glasgow (Blackie) and New York (Halsted Press), 1985. x + 328 pp., 246 figs., 2 coloured geological maps. Price £65, Mineralogical Magazine, 50(356), 351–351, doi:10.1180/minmag.1986.050.356.30, 1986.

Parada, M., Lopez-Escobar, L., Oliveros, V., Fuentes, F. and Morata, D.: Andean Magmatism., in The Geology of Chile, pp. 115–146, The Geological Society of London., n.d.

Parada, M. A., Feraud, G., Fuentes, F., Aguirre, L., Morata, D. and Larrondo, P.: Ages and cooling history of the Early Cretaceous Caleu pluton: testimony of a switch from a rifted to a compressional continental margin in central Chile, J. Geol. Soc., 162, 273–287, doi:10.1144/0016-764903-173, 2005.

Pearce, J. and Norry, M.: Petrogenetic Implications of Ti, Zr, Y, and Nb Variations in Volcanic-Rocks, Contrib. Mineral. Petrol., 69(1), 33–47, doi:10.1007/BF00375192, 1979.

Powell, R.: Inversion of the Assimilation and Fractional Crystallization (afc) Equations - Characterization of Contaminants from Isotope and Trace-Element Relationships in Volcanic Suites, J. Geol. Soc., 141(MAY), 447–452, doi:10.1144/gsjgs.141.3.0447, 1984.

Prouteau, G. and Scaillet, B.: Experimental constraints on the origin of the 1991 Pinatubo dacite, J. Petrol., 44(12), 2203–2241, doi:10.1093/petrology/egg075, 2003.

Rapp, R.: Amphibole-Out Phase-Boundary in Partially Melted Metabasalt, Its Control Over Liquid Fraction and Composition, and Source Permeability, J. Geophys. Res.-Solid Earth, 100(B8), 15601–15610, doi:10.1029/95JB00913, 1995a.

Rapp, R. P.: Amphibole-out phase boundary in partially melted metabasalt, its control over liquid fraction and composition, and source permeability, Journal of Geophysical Research: Solid Earth, 100(B8), 15601–15610, doi:10.1029/95JB00913, 1995b.

Ridolfi, F. and Renzulli, A.: Calcic amphiboles in calc-alkaline and alkaline magmas: thermobarometric and chemometric empirical equations valid up to 1,130°C and 2.2 GPa, Contributions to Mineralogy and Petrology, 163, 877–895, doi:10.1007/s00410-011-0704-6, 2012.

de Saint Blanquat, M., Horsman, E., Habert, G., Morgan, S., Vanderhaeghe, O., Law, R. and Tikoff, B.: Multiscale magmatic cyclicity, duration of pluton construction, and the paradoxical relationship between tectonism and plutonism in continental arcs, Tectonophysics, 500(1–4), 20–33, doi:10.1016/j.tecto.2009.12.009, 2011.

de Saint-Blanquat, M., Law, R. D., Bouchez, J. L. and Morgan, S. S.: Internal structure and emplacement of the Papoose Flat pluton: An integrated structural, petrographic, and magnetic susceptibility study, Geol. Soc. Am. Bull., 113(8), 976–995, doi:10.1130/0016-

Solid Earth Discuss., https://doi.org/10.5194/se-2019-43
Manuscript under review for journal Solid Earth
Discussion started: 27 March 2019

7606(2001)113<0976:ISAEOT>2.0.CO;2, 2001.

Sempere, T., Carlier, G., Soler, P., Fornari, M., Carlotto, V., Jacay, J., Arispe, O., Neraudeau, D., Cardenas, J., Rosas, S. and Jimenez, N.: Late Permian-Middle Jurassic lithospheric thinning in Peru and Bolivia, and its bearing on Andean-age tectonics, Tectonophysics, 345(1–4), 153–181, doi:10.1016/S0040-1951(01)00211-6, 2002.

Shackleton, R.M., Ries, A.C., Coward, M.P., Cobbold, P.R.: Structure, metamorphism and geochronology of the Arequipa Massif of coastal Peru, Journal of the Geological Society, 136, 195–214, 1979.

Sisson, T. and Layne, G.: H2o in Basalt and Basaltic Andesite Glass Inclusions from 4 Subduction-Related Volcanos, Earth Planet. Sci. Lett., 117(3–4), 619–635, doi:10.1016/0012-821X(93)90107-K, 1993.

Smith, A. L., Schellekens, J. H. and Díaz, A.-L. M.: Batholiths as markers of tectonic change in the northeastern Caribbean, in Special Paper 322: Tectonics and Geochemistry of the Northeastern Caribbean, vol. 322, pp. 99–122, Geological Society of America., 1998.

Somoza, R. and Zaffarana, C. B.: Mid-Cretaceous polar standstill of South America, motion of the Atlantic hotspots and the birth of the Andean cordillera, Earth Planet. Sci. Lett., 271(1–4), 267–277, doi:10.1016/j.epsl.2008.04.004, 2008.

Spera, F. J. and Bohrson, W. A.: Energy-constrained open-system magmatic processes I: General model and energy-constrained assimilation and fractional crystallization (EC-AFC) formulation, J. Petrol., 42(5), 999–1018, doi:10.1093/petrology/42.5.999, 2001.

Stewart, J. W.: Geología - Cuadrangulo de Mollendo (34r) y La Joya (34s), calameo.com [online] Available from: https://www.calameo.com/books/0008201299ceeee304f7d (Accessed 28 February 2019), 1968.

Sun, S. -s. and McDonough, W. F.: Chemical and isotopic systematics of oceanic basalts: implications for mantle composition and processes, Geological Society, London, Special Publications, 42(1), 313–345, doi:10.1144/GSL.SP.1989.042.01.19, 1989.

Tepper, J. H., Nelson, B. K., Bergantz, G. W. and Irving, A. J.: Petrology of the Chilliwack batholith, North Cascades, Washington: generation of calc-alkaline granitoids by melting of mafic lower crust with variable water fugacity, Contr. Mineral. and Petrol., 113(3), 333–351, doi:10.1007/BF00286926, 1993.

Tilton, G. and Barreiro, B.: Origin of Lead in Andean Calc-Alkaline Lavas, Southern Peru, Science, 210(4475), 1245–1247, doi:10.1126/science.210.4475.1245, 1980.

Voshage, H., Hofmann, A., Mazzucchelli, M., Rivalenti, G., Sinigoi, S., Raczek, I. and Demarchi, G.: Isotopic Evidence from the Ivrea Zone for a Hybrid Lower Crust Formed by Magmatic Underplating, Nature, 347(6295), 731–736, doi:10.1038/347731a0, 1990.

TABLE CAPTION

Table 1: Characteristics of the main mineral phases encountered in the Arequipa batholith.

FIGURE CAPTIONS

Solid Earth Discuss., https://doi.org/10.5194/se-2019-43
Manuscript under review for journal Solid Earth
Discussion started: 27 March 2019

Solid Earth
Discussions
Open Access

Figure 1: Geological map of the Coastal Batholith section in the Arequipa vicinity. ASF: Agua Salada Fault; LFS: Lluclla Fault System; CF: Cenicienta Fault.

Figure 2: Photomicrographs of thin sections (a) Small rounded pyroxenes in a plagioclase matrix (09SD43); (b) Residual pyroxene cores in amphibole grain (09SD33)

Figure 3: a) Amphibole compositions. Na+K (afpu) content vs. Si (afpu) diagram. The chemical data define two trends; amphiboles from the Gabbro and Diorites and Tiabaya units define the less Si-enriched trend and amphiboles from the Linga and Yarabamba units define the more Si-enriched trend. This highlights the general depletion in Si and alkaline in the amphibole spectrum. (GDU: Gabbros and Diorites unit, TU: Tiabaya unit, LU: Linga unit, YU : Yarabamba unit). b) Biotite compositions. Al (afpu) content vs. XMg diagram. We observe an unequal distribution of the biotites in the diagram with two groups, non-linked to the rock types. The distribution is correlated with the location of the sample; biotites with Al (apfu)>2.5 belong the Gabbro and Diorite unit and Tiabaya units, whereas biotites with Al (apfu)<2.5 belong to the Linga and Yarabamba units.

Figure 4: Pressure vs. temperature binary diagram for thermobarometric data issue from the analysis of amphiboles from the Arequipa batholith. G&D.U: Gabbros and Diorites unit, T. U: Tiabaya unit, L. U: Linga unit, Y. U : Yarabamba unit. BST: basement sample.

Figure 5: a) Total alkali vs Silica diagram for the rocks of the Arequipa's batholith. Blue diamonds: Jurassic rocks; green squares: Cretaceous rocks; orange triangles: Maastrichitan-Paleocene rocks. Domains from Cox et al. (1979). b) AFM diagram. Blue symbols: Jurassic rocks; green symbols: cretaceous rocks; orange symbols: maastrichitan-paleocene rocks. c) A/NK vs. A/CNK diagram. Blue symbols: Jurassic rocks; green symbols: cretaceous rocks; orange symbols: maastrichtian-paleocene rocks.

Figure 6: a) Chondrites normalized REE patterns of the plutonic rocks of the Arequipa batholith for the different facies (Anders & Grevesse, 1989). The domain of the Andean rocks is indicated in grey. b) Trace element spider diagram for the plutonic rocks of the Arequipa batholith (Sun &McDonough, 1989). The domain of the Andean rocks is indicated in grey.

Solid Earth Discuss., https://doi.org/10.5194/se-2019-43
Manuscript under review for journal Solid Earth
Discussion started: 27 March 2019

Figure 7: Rb-Sr isochron diagram for the plutonic rocks of the Arequipa batholith. Symbols are the same as in figure 4.

Figure 8: Sm-Nd isochron diagram for the plutonic rocks of the Arequipa batholith. Symbols are the same as in figure 4.

Figure 9: εNd values vs. $^{87}Sr/^{86}Sr_i$ ratios for the plutonic rocks of the Arequipa batholith. Symbols are the same as in figure 4.

Figure 10: Schematic cross section of the northwestern area of the Arequipa Batholith. LFS: Lluclla Fault System, CF: Cenicienta Fault, ASF: Aguasalada fault. The LFS separates the batholith into two parts: (i) a northeastern part made of the Gabbros & Diorites unit, the Tiabaya unit, the precambian basement and the Early Jurassic sedimentary strata (b) a southwestern part made up of the large Linga unit made of an amalgamation of several laccolith shaped intrusions crosscutting the Jurassic sedimentary strata.

Figure 11: $^{87}Sr/^{86}Sr_i$, $^{143}Nd/^{144}Nd_i$ ratios, Lu and Sr concentrations, all plotted versus Zr concentrations.

Supplementary files:

Supplement A: Coordinates of the 100 samples issued from the Arequipa section of the Southern Coastal batholith of Peru

Supplement B: Thermobarometric data for selected samples from the Arequipa batholith. Calculations based on the model from Ridolfi and Renzulli (2012).

Supplement C: Major and trace elements for 100 samples issued from the Arequipa batholith section.

Supplement D: Isotopic data and Rb, Sr, Sm, Nd abundances for selected samples from the Arequipa batholith section.

Solid Earth Discuss., https://doi.org/10.5194/se-2019-43
Manuscript under review for journal Solid Earth
Discussion started: 27 March 2019

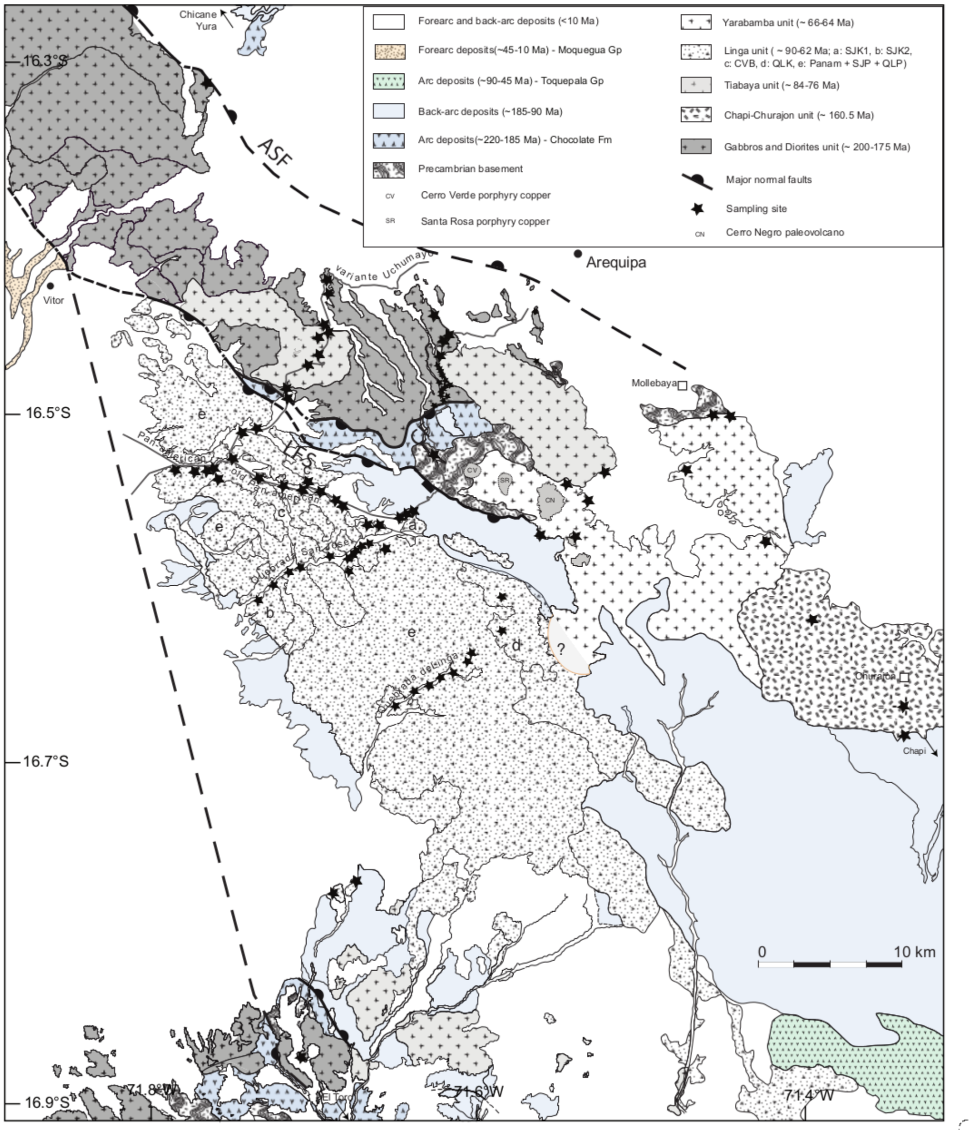

960

961 Figure 1

962

963

Solid Earth Discuss., https://doi.org/10.5194/se-2019-43
Manuscript under review for journal Solid Earth
Discussion started: 27 March 2019

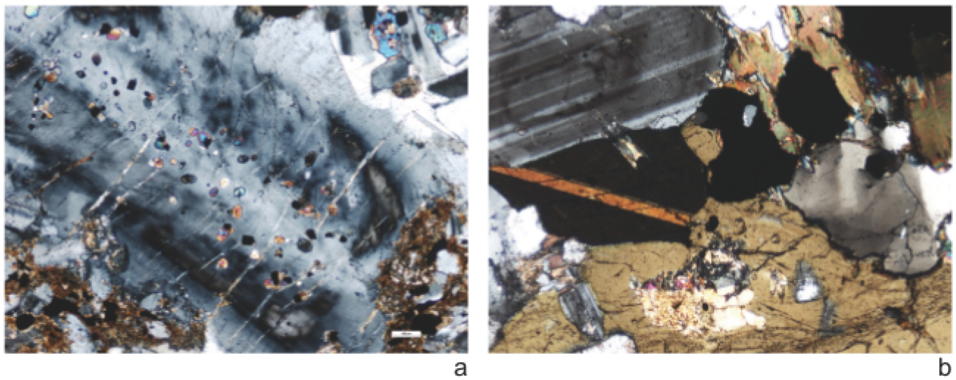

Figure 2

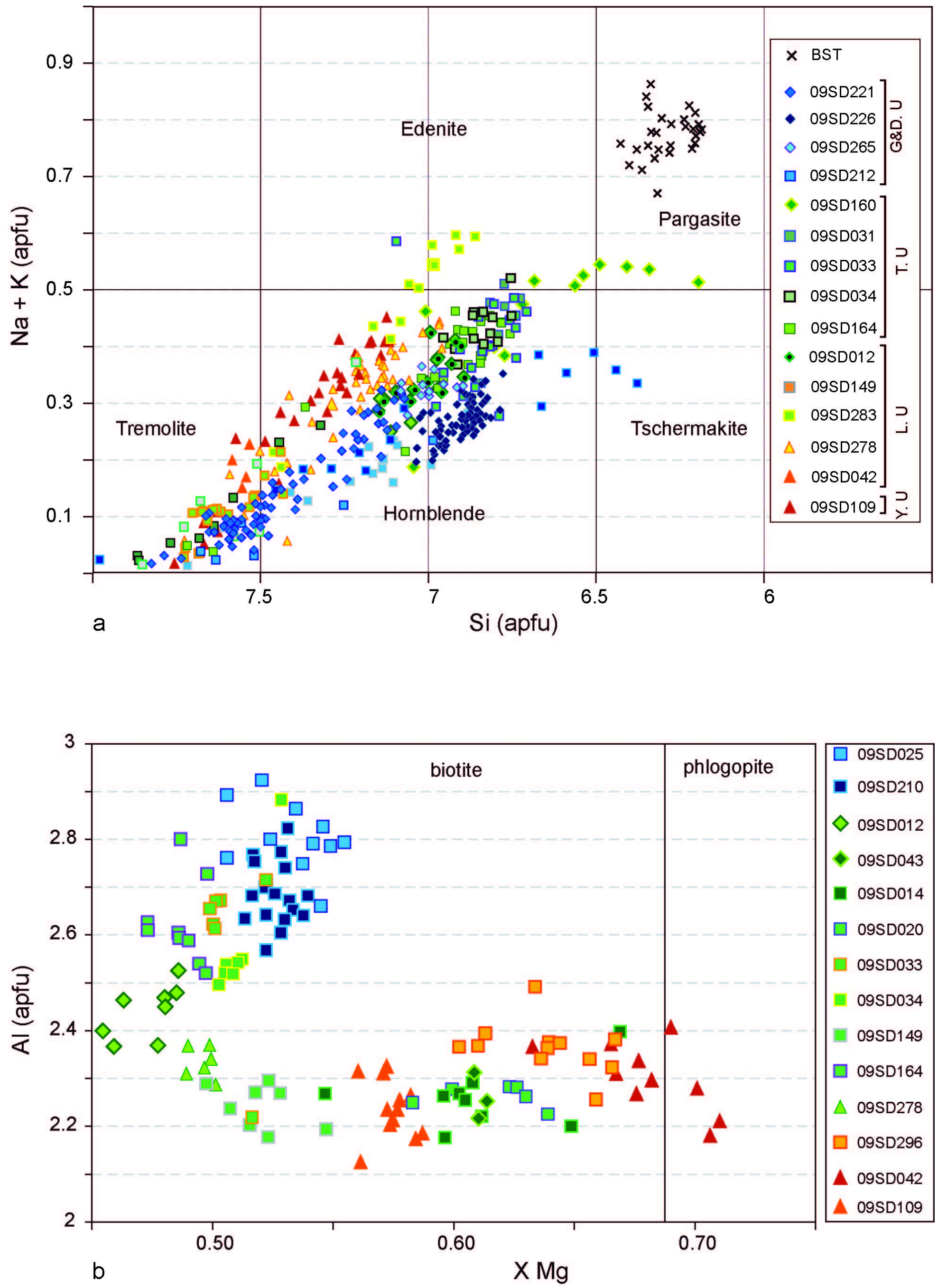

966

967 Figure 3

Solid Earth Discuss., https://doi.org/10.5194/se-2019-43
Manuscript under review for journal Solid Earth
Discussion started: 27 March 2019

Solid Earth Discussions

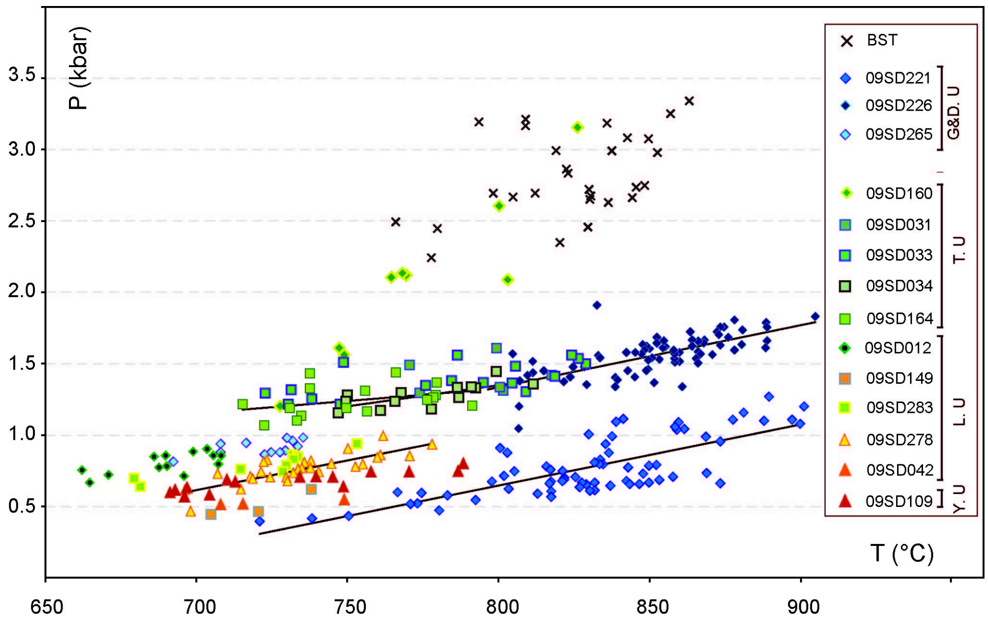

968

969 Figure 4

Solid Earth Discuss., https://doi.org/10.5194/se-2019-43
Manuscript under review for journal Solid Earth
Discussion started: 27 March 2019

Solid Earth
Discussions
Open Access
EGU

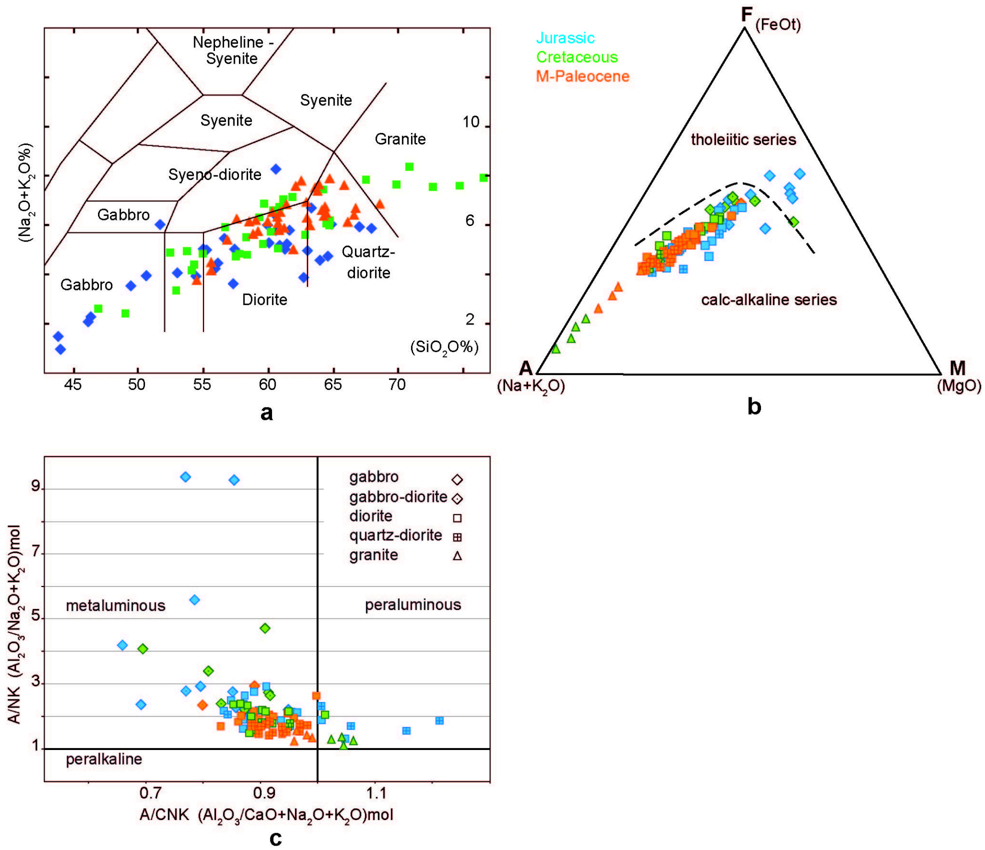

Figure 5

Solid Earth Discuss., https://doi.org/10.5194/se-2019-43
Manuscript under review for journal Solid Earth
Discussion started: 27 March 2019

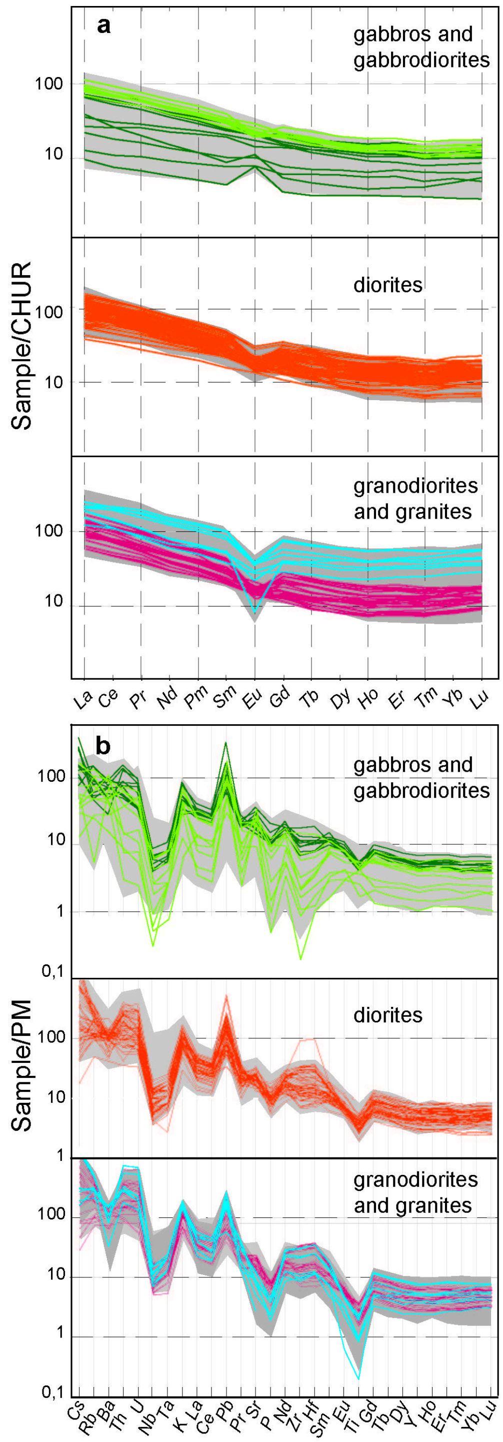

Figure 6

Solid Earth Discuss., https://doi.org/10.5194/se-2019-43
Manuscript under review for journal Solid Earth
Discussion started: 27 March 2019

Solid Earth
Discussions

974

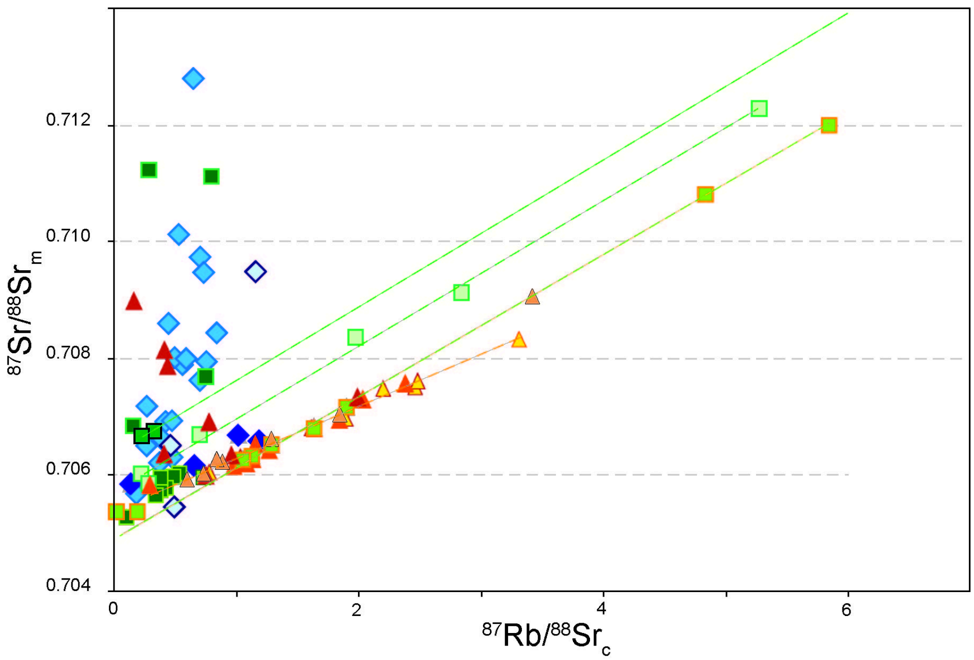

975

976

977 Figure 7

978

979

Solid Earth Discuss., https://doi.org/10.5194/se-2019-43
Manuscript under review for journal Solid Earth
Discussion started: 27 March 2019

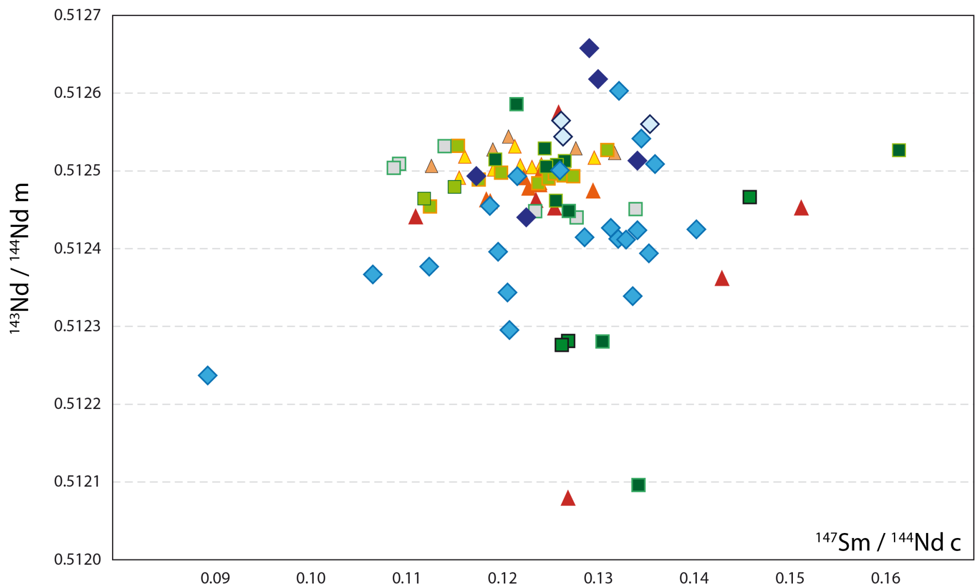

980

981 Figure 8

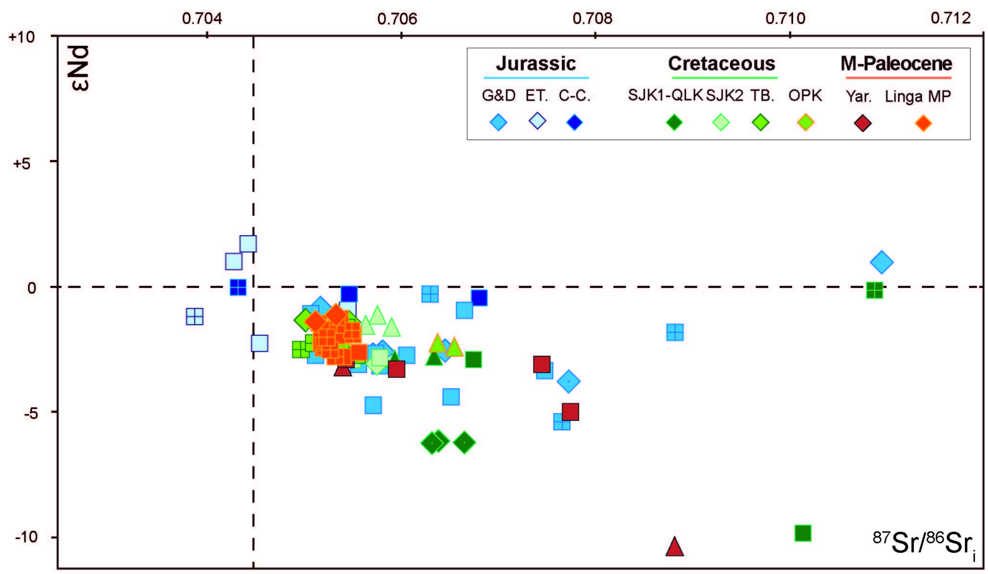

982

983 Figure 9

984

Solid Earth Discuss., https://doi.org/10.5194/se-2019-43
Manuscript under review for journal Solid Earth
Discussion started: 27 March 2019

Solid Earth
Discussions
Open Access
EGU

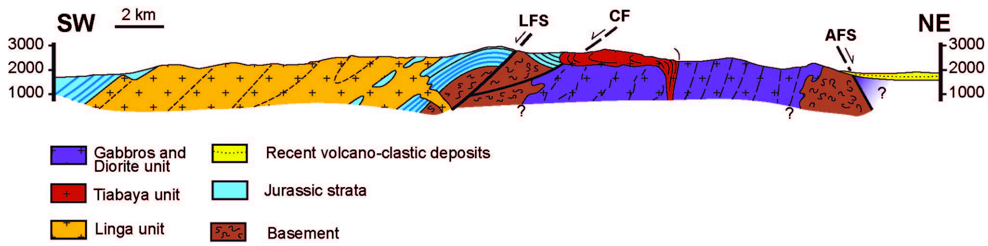

Figure 10

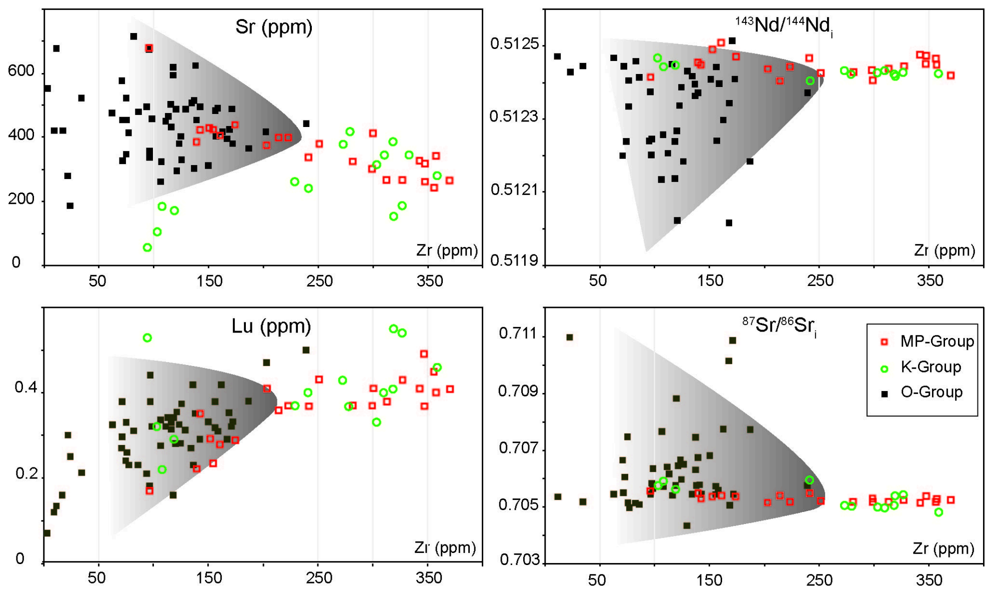

Figure 11

	Mineral phase	occurrence	composition
quartz and feldspar	quartz	interstitials grains and/or subhedral rounded crystal up to 2-3 mm in diameter	
	plagioclase	in every rock type with various habits, mainly as euhedral grains, either with grain size similar to the other minerals of the rock or as plurimillimeter-sized phenocrysts. Twins and zonations are ubiquitous. It generally exhibits normal zoning with sodic rims	An-content range is An_{92}-An43 for the gabbros and An_{53}-An_{17} for the granites
	alkali feldspar	in the felsic rocks - appears as anhedral, more or less perthitic grains in the groundmass as plurimillimeter-sized phenocrysts	Or_{99} to Or_{79}
Ferro-magnesians	pyroxene	in the mafic rocks (gabbro to diorite) and does not exceed 5 vol.% except for the gabbrodiorites of the Linga unit. It occurs both as isolated euhedral grains and more rarely as small rounded grains included into plagioclases (Figure 3a) in the mafic rocks (gabbro and gabbrodiorites). In the diorites, the pyroxene occurs as inclusion in the core of amphibole grains (Figure 3 b) The orthopyroxene is only present in the most mafic samples of the Linga unit (09SD12 and 09SD43) Clinopyroxene occurs in association with the orthopyroxene except in the more differenciated rocks devoid of orthopyroxene.	ranging from 52-61 mol % En, 36-45 mol % Fs and 2-3 mol % Wo compositions are quite homogeneous between Linga and Tiabaya (29-46 mol % En, 11-27 mol % Fs and 35-50 mol % Wo).
	amphibole	Green or brown amphibole is ubiquitous except for the Chapi-Churajón unit. It occurs as small to large-sized (up to 5 mm) euhedral grains, sometimes with inclusions of accessory minerals or plagioclase and twins features	amphiboles are calcic with CaO content >9.5 wt%. They are pargasite, tschermakite or magnesiohornblende in the mafic rocks, and edenite, hornblende or tremolite in the intermediate and felsic rocks (Figure 5).
	biotite	small to large (up to 5 mm) subhedral or euhedral crystals with various inclusions of accessory phases as Fe-Ti oxyde, zircon and apatite. It constitutes up to 10-15 vol % of the mode of the different lithologies.	large range of XMg (0.45-0.71) for a limited Al_2O_3 range (12-16 wt%)
accessory minerals	zircon	commonly found in the sample set and therefore was used for U-Pb dating. It occurs as prismatic bipyramidal, euhedral and highly transparent to slightly pink in color. The zircon sizes vary between 150 and 400 μm in length. Cathodoluminescence imaging shows that oscillatory zoning is prominent in the zircon population, and inherited cores occur in several samples.	
	fluoroapatite	small prismatic crystals and are commonly found as inclusions in biotite and plagioclase, in gabbrodiorite to granitic facies.	41-43 wt% P_2O_5, 50-56 wt% CaO and 1.6-3.2 wt% F
	epidote	rare and small-sized isolated grains in the mafic to intermediate rocks.	
	titanite	not present in all of our sample set but occurs in all lithological types. It is abundant in some diorites and quartz-diorites (up to 2 vol% of the mode). It occurs mostly as isolated euhedral crystals, sometimes twinned and associated with hematite Fe-Ti oxydes. Its chemical composition remains homogeneous between the facies	(TiO_2 range: 36.4-39.8 % ox.) but in the granites with slightly lower TiO_2 values (TiO_2: 34.6-38.4 % ox.).
	oxydes	ubiquitous in all the rocks, and occur mainly as squared-euhedral crystal grains of magnetite and ilmenite, isolated or associated with ferro-magnesian phases. Hematite also occurs preferentially in the mafic rocks, and is sometimes affected by titanite veins. Ilmenite is found in association with hematite. Oxydes in general constitute less than 5 vol% of the mode of the rocks, mostly in the mafic lithologies, especially in the Gabbros and Diorites unit.	

Table 1